CHAPTER

Radial Flow Gas Turbines

8

I like work; it fascinates me, I can sit and look at it for hours.
Jerome K. Jerome, *Three Men in a Boat*

8.1 INTRODUCTION

The radial flow turbine has had a long history of development being first conceived for the purpose of producing hydraulic power over 180 years ago. A French engineer, Fourneyron, developed the first commercially successful hydraulic turbine (circa 1830) and this was of the *radial-outflow* type. A *radial-inflow* type of hydraulic turbine was built by Francis and Boyden in the United States (circa 1847), which gave excellent results and was highly regarded. This type of machine is now known as the *Francis turbine*, a simplified arrangement of it being shown in Figure 1.1. It will be observed that the flow path followed is from the radial direction to what is substantially an axial direction. A flow path in the reverse direction (radial outflow), for a single-stage turbine anyway, creates several problems, one of which (discussed later) is low specific work. However, as pointed out by Shepherd (1956) radial-outflow steam turbines comprising many stages have received considerable acceptance in Europe. Figure 8.1 from Kearton (1951) shows diagrammatically the *Ljungström steam turbine*, which, because of the tremendous increase in the specific volume of steam, makes the radial-outflow flow path virtually imperative. A unique feature of the Ljungström turbine is that it does not have any stationary blade rows. The two rows of blades constituting each of the stages rotate in opposite directions so that they can both be regarded as rotors.

The inward-flow radial (IFR) turbine covers tremendous ranges of power, rates of mass flow, and rotational speeds, from very large Francis turbines used in hydroelectric power generation and developing hundreds of megawatts (see Figures 9.12 and 9.13) down to tiny closed cycle gas turbines for space power generation of a few kilowatts.

The IFR gas turbine has been, and continues to be, used extensively for powering automotive turbocharges, aircraft auxiliary power units, expansion units in gas liquefaction, and other cryogenic systems and as a component of the small (10 kW) gas turbines used for space power generation (Anon., 1971). It has been considered for primary power use in automobiles and in helicopters. According to Huntsman, Hudson, and Hill (1992), studies at Rolls-Royce have shown that a cooled, high efficiency IFR turbine could offer significant improvement in performance as the gas generator turbine of a high technology turboshaft engine. What is needed to enable this type of application are some small improvements in current technology levels. However, designers of this new generation

DOI: 10.1016/B978-1-85617-793-1.00008-0

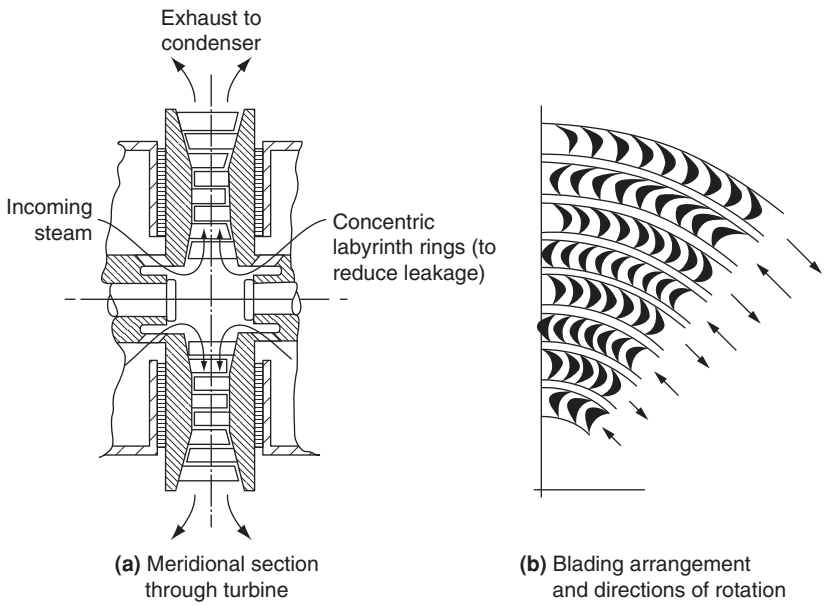

FIGURE 8.1

Ljungström Type Outward Flow Radial Turbine (Adapted from Kearton, 1951)

of IFR turbines face considerable problems, particularly in the development of advanced techniques of rotor cooling or of ceramic, shock-resistant rotors.

As indicated later in this chapter, over a limited range of specific speed, IFR turbines provide an efficiency about equal to that of the best axial-flow turbines. The significant advantages offered by the IFR turbine compared with the axial-flow turbine is the greater amount of work that can be obtained per stage, the ease of manufacture, and its superior ruggedness.

8.2 TYPES OF INWARD-FLOW RADIAL TURBINE

In the centripetal turbine energy is transferred from the fluid to the rotor in passing from a large radius to a small radius. For the production of positive work the product of Uc_θ at entry to the rotor must be greater than Uc_θ at rotor exit [eqn. (1.18c)]. This is usually arranged by imparting a large component of tangential velocity at rotor entry, using single or multiple nozzles, and allowing little or no swirl in the exit absolute flow.

Cantilever Turbine

Figure 8.2(a) shows a *cantilever* IFR turbine where the blades are limited to the region of the rotor tip, extending from the rotor in the *axial* direction. In practice the cantilever blades are usually of the impulse type (i.e., low reaction), by which it is implied that there is little change in relative velocity

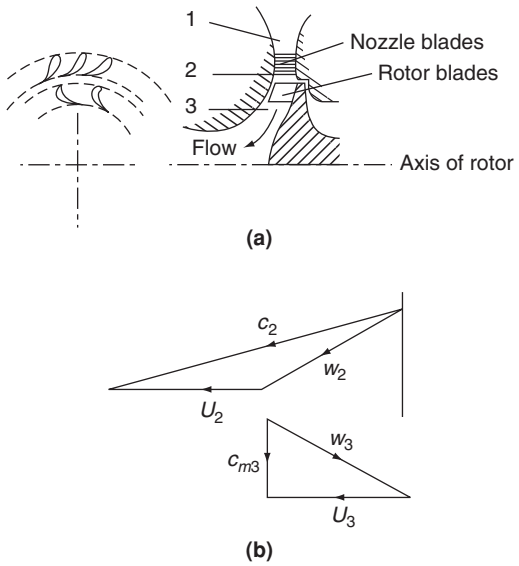

FIGURE 8.2

Arrangement of Cantilever Turbine and Velocity Triangles at the Design Point

at inlet and outlet of the rotor. There is no fundamental reason why the blading should not be of the reaction type. However, the resulting expansion through the rotor would require an increase in flow area. This extra flow area is extremely difficult to accommodate in a small radial distance, especially as the radius decreases through the rotor row.

Aerodynamically, the cantilever turbine is similar to an axial-impulse turbine and can even be designed by similar methods. Figure 8.2(b) shows the velocity triangles at rotor inlet and outlet. The fact that the flow is radially inwards hardly alters the design procedure because the blade radius ratio r_2/r_3 is close to unity anyway.

The 90° IFR Turbine

Because of its higher structural strength compared with the cantilever turbine, the 90° IFR turbine is the preferred type. Figure 8.3 shows a typical layout of a 90° IFR turbine; the inlet blade angle is generally made zero, a fact dictated by the material strength and often high gas temperature. The rotor vanes are subject to high stress levels caused by the centrifugal force field, together with a pulsating and often unsteady gas flow at high temperatures. Despite possible performance gains the use of non-radial (or swept) vanes is generally avoided, mainly because of the additional stresses that arise due to bending. Nevertheless, despite this difficulty, Meitner and Glassman (1983) have considered designs using sweptback vanes in assessing ways of increasing the work output of IFR turbines.

From station 2 the rotor vanes extend radially inward and turn the flow into the axial direction. The exit part of the vanes, called the *exducer*, is curved to remove most if not all of the absolute tangential component of velocity. The 90° IFR turbine or centripetal turbine is very similar in appearance to the centrifugal compressor of Chapter 7, but with the flow direction and blade motion reversed.

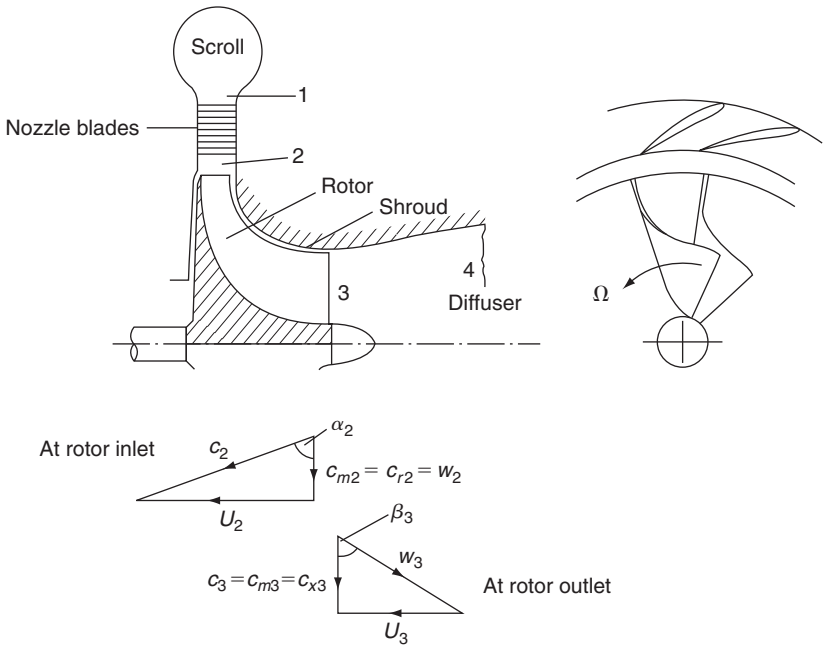

FIGURE 8.3

Layout and Velocity Diagrams for a 90° Inward-Flow Radial Turbine at the Nominal Design Point

The fluid discharging from the turbine rotor may have a considerable velocity c_3 and an axial diffuser (see Chapter 7) would normally be incorporated to recover most of the kinetic energy, $\frac{1}{2}c_3^2$, which would otherwise be wasted. In hydraulic turbines (discussed in Chapter 9) a diffuser is invariably used and is called the *draught tube*.

In Figure 8.3 the velocity triangles are drawn to suggest that the inlet relative velocity, w_2, is *radially* inward, i.e., zero incidence flow, and the absolute flow at rotor exit, c_3, is axial. This configuration of the velocity triangles, popular with designers for many years, is called the *nominal design* condition and will be considered in some detail in the following pages. Following this the so-called optimum efficiency design will be explained.

8.3 THERMODYNAMICS OF THE 90° IFR TURBINE

The complete adiabatic expansion process for a turbine comprising a nozzle blade row, a radial rotor followed by a diffuser, corresponding to the layout of Figure 8.3, is represented by the Mollier diagram shown in Figure 8.4. In the turbine, frictional processes cause the entropy to increase in all components and these irreversibilities are implied in Figure 8.4.

Across the nozzle blades the stagnation enthalpy is assumed constant, $h_{01} = h_{02}$ and, therefore, the static enthalpy drop is

$$h_1 - h_2 = \frac{1}{2}(c_2^2 - c_1^2), \tag{8.1}$$

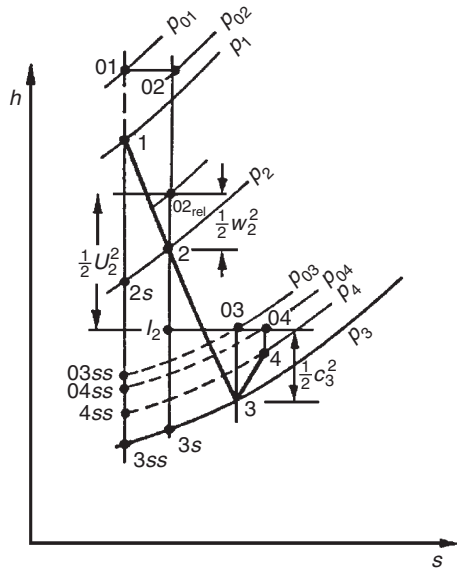

FIGURE 8.4

Mollier Diagram for a 90° Inward-Flow Radial Turbine and Diffuser (At the Design Point)

corresponding to the static pressure change from p_1 to the lower pressure p_2. The *ideal* enthalpy change ($h_1 - h_{2s}$) is between these *same* two pressures but at constant entropy.

In Chapter 7 it was shown that the rothalpy, $I = h_{0,\text{rel}} - \frac{1}{2}U^2$, is constant for an adiabatic irreversible flow process, relative to a rotating component. For the rotor of the 90° IFR turbine,

$$h_{02,\text{rel}} - \frac{1}{2}U_2^2 = h_{03,\text{rel}} - \frac{1}{2}U_3^2.$$

Thus, as $h_{0,\text{rel}} - \frac{1}{2}w^2$,

$$h_2 - h_3 = \frac{1}{2}[(U_2^2 - U_3^2) - (w_2^2 - w_3^2)]. \tag{8.2a}$$

In this analysis the reference point 2 (Figure 8.3) is taken to be at the inlet radius r_2 of the rotor (the blade tip speed $U_2 = \Omega r_2$). This implies that the nozzle irreversibilities are lumped together with any friction losses occurring in the annular space between nozzle exit and rotor entry (usually scroll losses are included as well).

Across the diffuser the stagnation enthalpy does not change, $h_{03} = h_{04}$, but the static enthalpy *increases* as a result of the velocity diffusion. Hence,

$$h_4 - h_3 = \frac{1}{2}\left(c_3^2 - c_4^2\right). \tag{8.3}$$

The specific work done by the fluid on the rotor is

$$\Delta W = h_{01} - h_{03} = U_2 c_{\theta 2} - U_3 c_{\theta 3}. \tag{8.4a}$$

As $h_{01} = h_{02}$,

$$\Delta W = h_{02} - h_{03} = h_2 - h_3 + \frac{1}{2}(c_2^2 - c_3^2) = \frac{1}{2}[(U_2^2 - U_3^2) - (w_2^2 - w_3^2) + (c_2^2 - c_3^2)] \tag{8.4b}$$

after substituting eqn. (8.2a).

8.4 BASIC DESIGN OF THE ROTOR

Each term in eqn. (8.4b) makes a contribution to the specific work done on the rotor. A significant contribution comes from the first term, namely, $\frac{1}{2}(U_2^2 - U_1^2)$, and is the main reason why the inward-flow turbine has such an advantage over the outward-flow turbine where the contribution from this term would be negative. For the axial-flow turbine, where $U_2 = U_1$, of course, no contribution to the specific work is obtained from this term. For the second term in eqn. (8.4b) a positive contribution to the specific work is obtained when $w_3 > w_2$. In fact, accelerating the relative velocity through the rotor is a most useful aim of the designer as this is conducive to achieving a low loss flow. The third term in eqn. (8.4b) indicates that the absolute velocity at rotor inlet should be larger than at rotor outlet so as to increase the work input to the rotor. With these considerations in mind the general shape of the velocity diagram shown in Figure 8.3 results.

Nominal Design

The *nominal design* is defined by a relative flow of zero incidence at rotor inlet (i.e., $w_2 = c_{r2}$) and an absolute flow at rotor exit, which is axial (i.e., $c_3 = c_{x3}$).[1] Thus, from eqn. (8.4a), with $c_{\theta 3} = 0$ and $c_{\theta 2} = U_2$, the specific work for the nominal design is simply

$$\Delta W = U_2^2. \tag{8.4c}$$

Example 8.1

The rotor of an IFR turbine, which is designed to operate at the nominal condition, is 23.76 cm in diameter and rotates at 38,140 rev/min. At the design point the absolute flow angle at rotor entry is 72°. The rotor mean exit diameter is one half of the rotor diameter and the relative velocity at rotor exit is twice the relative velocity at rotor inlet.

Determine the relative contributions to the specific work of each of the three terms in eqn. (8.4b).

Solution

The blade tip speed is $U_2 = \pi N D_2/60 = \pi \times 38{,}140 \times 0.2376/60 = 474.5$ m/s.

Referring to Figure 8.3, $w_2 = U_2 \cot \alpha_2 = 154.17$ m/s, and $c_2 = U_2/\sin \alpha_2 = 498.9$ m/s.

$$c_3^2 = w_3^2 - U_3^2 = (2 \times 154.17)^2 - \left(\frac{1}{2} \times 474.5\right)^2 = 38{,}786\ \mathrm{m^2/s^2}.$$

[1] This arrangement ($c_{\theta 3} = 0$) minimizes the exit kinetic energy loss. However, some designers may opt for some exit swirl in the flow in order to benefit a subsequent diffusion process.

Hence,

$$(U_2^2 - U_2^2) = U_2^2(1 - 1/4) = 168,863\,\mathrm{m}^2/\mathrm{s}^2,$$

$$w_3^2 - w_2^2 = 3 \times w_2^2 = 71,305\,\mathrm{m}^2/\mathrm{s}^2$$

and

$$c_2^2 - c_3^2 = 210,115\,\mathrm{m}^2/\mathrm{s}^2.$$

Thus, summing the values of the three terms and dividing by 2, we get $\Delta W = 225{,}142\,\mathrm{m}^2/\mathrm{s}^2$.

The fractional inputs from each of the three terms are, for the U^2 terms, 0.375; for the w^2 terms, 0.158; for the c^2 terms, 0.467.

Finally, as a numerical check, the specific work is, $\Delta W = U_2^2 = 474.5^2 = 225,150\,\mathrm{m}^2/\mathrm{s}^2$, which, apart from some rounding errors, agrees with the preceding computations.

Spouting Velocity

The term *spouting velocity* c_0 (originating from hydraulic turbine practice) is defined as that velocity that has an associated kinetic energy equal to the isentropic enthalpy drop from turbine inlet stagnation pressure p_{01} to the final exhaust pressure. The exhaust pressure here can have several interpretations depending upon whether total or static conditions are used in the related efficiency definition and upon whether or not a diffuser is included with the turbine. Thus, when *no* diffuser is used

$$\frac{1}{2}c_0^2 = h_{01} - h_{03ss} \tag{8.5a}$$

or

$$\frac{1}{2}c_0^2 = h_{01} - h_{3ss} \tag{8.5b}$$

for the total and static cases, respectively.

In an *ideal* (frictionless) radial turbine with complete recovery of the exhaust kinetic energy and with $c_{\theta 2} = U_2$,

$$\Delta W = U_2^2 = \frac{1}{2}c_0^2$$

therefore,

$$\frac{U_2}{c_0} = 0.707.$$

At the best efficiency point of actual (frictional) 90° IFR turbines it is found that this velocity ratio is, generally, in the range $0.68 < U_2/c_0 < 0.71$.

8.5 NOMINAL DESIGN POINT EFFICIENCY

Referring to Figure 8.4, the total-to-static efficiency in the absence of a diffuser is defined as

$$\eta_{ts} = \frac{h_{01} - h_{03}}{h_{01} - h_{3ss}} = \frac{\Delta W}{\Delta W + \frac{1}{2}c_3^2 + (h_3 - h_{3s}) + (h_{3s} - h_{3ss})}. \tag{8.6}$$

The passage enthalpy losses can be expressed as a fraction (ζ) of the exit kinetic energy relative to the nozzle row and the rotor, i.e.,

$$h_3 - h_{3s} = \frac{1}{2}w_3^2\zeta_R, \tag{8.7a}$$

$$h_{3s} - h_{3ss} = \frac{1}{2}c_2^2\zeta_N(T_3/T_2) \tag{8.7b}$$

for the rotor and nozzles, respectively. It is noted that, for a constant pressure process, $\mathrm{d}s = \mathrm{d}h/T$, hence, the approximation,

$$h_{3s} - h_{3ss} = (h_2 - h_{2s})(T_3/T_2).$$

Substituting for the enthalpy losses in eqn. (8.6),

$$\eta_{ts} = \left[1 + \frac{1}{2}(c_3^2 + w_3^3\zeta_R + c_2^2\zeta_N T_3/T_2)/\Delta W\right]^{-1}. \tag{8.8}$$

From the design point velocity triangles, Figure 8.3,

$$c_2 = U_2 \operatorname{cosec} a_2,\ w_3 = U_3 \operatorname{cosec}\beta_3,\ c_3 = U_3 \cot\beta_3,\ \Delta W = U_2^2.$$

Thus, substituting all these expressions in eqn. (8.8) and noting that $U_3 = U_2 r_3/r_2$,

$$\eta_{ts} = \left\{1 + \frac{1}{2}\left[\zeta_N \frac{T_3}{T_2}\operatorname{cosec}^2\alpha_2 + \left(\frac{r_3}{r_2}\right)^2(\zeta_R \operatorname{cosec}^2\beta_3 + \cot^2\beta_3)\right]\right\}^{-1}, \tag{8.9a}$$

where r_3 and β_3 are taken to apply at the arithmetic mean radius, i.e., $r_3 = \frac{1}{2}(r_{3s} + r_{3h})$. Note that r_{3s} is the shroud radius at rotor exit and r_{3h} is the hub radius at rotor exit. The temperature ratio (T_3/T_2) in eqn. (8.9a) can be obtained as follows.

At the nominal design condition, referring to the velocity triangles of Figure 8.3, $w_3^2 - U_3^2 = c_3^2$, and so eqn. (8.2a) can be rewritten as

$$h_2 - h_3 = \frac{1}{2}(U_2^2 - w_2^2 + c_3^2). \tag{8.2b}$$

This particular relationship, in the form $I = h_{02,\mathrm{rel}} - \frac{1}{2}U_2^2 = h_{03}$, can be easily identified in Figure 8.4.

Again, referring to the velocity triangles, $w_2 = U_2 \cot\alpha_2$ and $c_3 = U_3 \cot\beta_3$, a useful alternative form to eqn. (8.2b) is obtained:

$$h_2 - h_3 = \frac{1}{2}U_2^2\left[(1 - \cot^2 a_2) + (r_3/r_2)\cot^2\beta_3\right], \tag{8.2c}$$

where U_3 is written as $U_2 r_3/r_2$. For a perfect gas the temperature ratio T_3/T_2 can be easily found. Substituting $h = C_p T = \gamma RT/(\gamma - 1)$ in eqn. (8.2c),

$$1 - \frac{T_3}{T_2} = \frac{1}{2} U_2^2 \frac{(\gamma - 1)}{\gamma R T_2} \left[1 - \cot^2 \alpha_2 + \left(\frac{r_3}{r_2} \right)^2 \cot^2 \beta_3 \right],$$

therefore,

$$\frac{T_3}{T_2} = 1 - \frac{1}{2}(\gamma - 1) \left(\frac{U_2}{a_2} \right)^2 \left[1 - \cot^2 \alpha_2 + \left(\frac{r_3}{r_2} \right)^2 \cot^2 \beta_3 \right], \tag{8.2d}$$

where $a_2 = (\gamma R T_2)^{1/2}$ is the sonic velocity at temperature T_2.

Generally this temperature ratio will have only a very minor effect upon the numerical value of η_{ts} and so it is often ignored in calculations. Thus,

$$\eta_{ts} \simeq \left\{ 1 + \frac{1}{2} \left[\zeta_N \operatorname{cosec}^2 \alpha_2 + \left(\frac{r_3}{r_2} \right)^2 \left(\zeta_R \operatorname{cosec}^2 \beta_3 + \cos^2 \beta_3 \right) \right] \right\}^{-1} \tag{8.9b}$$

is the expression normally used to determine the total-to-static efficiency. An alternative form for η_{ts} can be obtained by rewriting eqn. (8.6) as

$$\eta_{ts} = \frac{h_{01} - h_{03}}{h_{01} - h_{3ss}} = \frac{(h_{01} - h_{3ss}) - (h_{03} - h_3) - (h_3 - h_{3s}) - (h_{3s} - h_{3ss})}{(h_{01} - h_{3ss})} = 1 - (c_3^2 + \zeta_N c_2^2 + \zeta_R w_3^2)/c_0^2, \tag{8.10}$$

where the spouting velocity c_0 is defined by

$$h_{01} - h_{3ss} = \frac{1}{2} c_0^2 = C_p T_{01} \left[1 - (p_3/p_{01})^{(\gamma - 1)/\gamma} \right]. \tag{8.11}$$

A simple connection exists between total-to-total and total-to-static efficiency, which can be obtained as follows. Writing

$$\Delta W = \eta_{ts} \Delta W_{is} = \eta_{ts} (h_{01} - h_{3ss})$$

then

$$\eta_{tt} = \frac{\Delta W}{\Delta W_{is} - \frac{1}{2} c_3^2} = \frac{1}{\frac{1}{\eta_{ts}} - \frac{c_3^2}{2 \Delta W}}.$$

Therefore,

$$\frac{1}{\eta_{tt}} = \frac{1}{\eta_{ts}} - \frac{c_3^2}{2 \Delta W} = \frac{1}{\eta_{ts}} - \frac{1}{2} \left(\frac{r_3}{r_2} \cot \beta_3 \right)^2. \tag{8.12}$$

Example 8.2

Performance data from the CAV type 01 radial turbine (Benson, Cartwright, and Das 1968) operating at a pressure ratio p_{01}/p_3 of 1.5 with zero incidence relative flow onto the rotor is presented in the following form:

$$\dot{m}\sqrt{T_{01}/p_{01}} = 1.44 \times 10^{-5}, \quad \text{ms(K)}^{1/2},$$

$$N/\sqrt{T_{01}} = 2410, \quad (\text{rev/min})/\text{K}^{1/2},$$

$$\tau/p_{01} = 4.59 \times 10^{-6}, \quad \text{m}^3,$$

where τ is the torque, corrected for bearing friction loss. The principal dimensions and angles, etc. are given as follows:

Rotor inlet diameter, 72.5 mm;
Rotor inlet width, 7.14 mm;
Rotor mean outlet diameter, 34.4 mm;
Rotor outlet annulus height, 20.1 mm;
Rotor inlet angle, 0°;
Rotor outlet angle, 53°;
Number of rotor blades, 10;
Nozzle outlet diameter, 74.1 mm;
Nozzle outlet angle, 80°;
Nozzle blade number, 15.

The turbine is "cold tested" with air heated to 400 K (to prevent condensation erosion of the blades). At nozzle outlet an estimate of the flow angle is given as 70° and the corresponding enthalpy loss coefficient is stated to be 0.065. Assuming that the absolute flow at rotor exit is without swirl and uniform and the relative flow leaves the rotor without any deviation, determine the total-to-static and overall efficiencies of the turbine, the rotor enthalpy loss coefficient and the rotor relative velocity ratio.

Solution

The data given are obtained from an actual turbine test and, even though the bearing friction loss has been corrected, there is an additional reduction in the specific work delivered due to disk friction and tip leakage losses, etc. The rotor speed $N = 2410\sqrt{400} = 48,200$ rev/min, the rotor tip speed $U_2 = \pi N D_2/60 = 183$ m/s and, hence, the specific work done by the rotor $\Delta W = U_2^2 = 33.48\,\text{kJ/kg}$. The corresponding isentropic total-to-static enthalpy drop is

$$h_{01} - h_{3ss} = C_p T_{01}\left[1 - (p_3/p_{01})^{(\gamma-1)/\gamma}\right] = 1.005 \times 400\left[1 - (1/1.5)^{1/3.5}\right] = 43.97\,\text{kJ/kg}.$$

Thus, the total-to-static efficiency is

$$\eta_{ts} = \Delta W/(h_{01} - h_{3ss}) = 76.14\%.$$

The actual specific work output to the shaft, after allowing for the bearing friction loss, is

$$\begin{aligned}\Delta W_{\text{act}} = \tau\Omega/\dot{m} &= \left(\frac{\tau}{p_{01}}\right)\frac{N}{\sqrt{T_{01}}}\left(\frac{p_{01}}{\dot{m}\sqrt{T_{01}}}\right)\frac{\pi}{30}T_{01} \\ &= 4.59 \times 10^{-6} \times 2410 \times \pi \times 400/(30 \times 1.44 \times 10^{-5}) \\ &= 32.18\ \text{kJ/kg}.\end{aligned}$$

Thus, the turbine overall total-to-static efficiency is

$$\eta_0 = \Delta W_{\text{act}}/(h_{01} - h_{3ss}) = 73.18\%.$$

By rearranging eqn. (8.9b) the rotor enthalpy loss coefficient can be obtained:

$$\begin{aligned}\zeta_R &= \left[2(1/\eta_{ts} - 1) - \zeta_N \operatorname{cosec}^2\alpha_2\right](r_2/r_3)^2 \sin^2\beta_3 - \cos^2\beta_3 \\ &= \left[2(1/0.7613 - 1) - 0.065 \times 1.1186\right] \times 4.442 \times 0.6378 - 0.3622 \\ &= 1.208.\end{aligned}$$

At rotor exit the absolute velocity is uniform and axial. From the velocity triangles, Figure 8.3,

$$w_3^2(r) = U_3^2 + c_3^2 = U_3^2\left[\left(\frac{r}{r_3}\right)^2 + \cot^2\beta_3\right],$$

$$w_2 = U_2 \cot\alpha_2,$$

ignoring blade-to-blade velocity variations. Hence,

$$\frac{w_3(r)}{w_2} = \frac{r_3}{r_2}\tan\alpha_2\left[\left(\frac{r}{r_3}\right)^2 + \cot^2\beta_3\right]^{1/2}. \tag{8.13}$$

The lowest value of this relative velocity ratio occurs when, $r = r_{3h} = (34.4 - 20.1)/2 = 7.15$ mm, so that

$$\frac{w_{3h}}{w_2} = 0.475 \times 2.904\left[0.415^2 + 0.7536^2\right]^{1/2} = 1.19.$$

The relative velocity ratio corresponding to the mean exit radius is

$$\frac{w_3}{w_2} = 0.475 \times 2.904\left[1 + 0.7536^2\right]^{1/2} = 1.73.$$

It is worth commenting that higher total-to-static efficiencies have been obtained in other small radial turbines operating at higher pressure ratios. Rodgers (1969) has suggested that total-to-static efficiencies in excess of 90% for pressure ratios up to 5 to 1 can be attained. Nusbaum and Kofskey (1969) reported an experimental value of 88.8% for a small radial turbine (fitted with an outlet diffuser, admittedly!) at a pressure ratio p_{01}/p_4 of 1.763. In the design point exercise just given the high rotor enthalpy loss coefficient and the corresponding relatively low total-to-static efficiency may well be related to the low relative velocity ratio determined on the hub. Matters are probably worse than this as the calculation is based only on a simple one-dimensional treatment. In determining velocity ratios across the rotor, account should also be taken of the effect of blade-to-blade velocity variation (outlined in this chapter) as well as viscous effects. The number of vanes in the rotor (10) may be insufficient on the basis of Jamieson's theory[2] (1955), which suggests 18 vanes (i.e., $Z_{\min} = 2\pi \tan\alpha_2$). For this turbine, at lower nozzle exit angles, eqn. (8.13) suggests that the relative velocity ratio becomes even less favourable despite the fact that the Jamieson blade spacing criterion is being approached. (For $Z = 10$, the optimum value of α_2 is about 58°.)

[2]Included later in this chapter.

8.6 MACH NUMBER RELATIONS

Assuming the fluid is a perfect gas, expressions can be deduced for the important Mach numbers in the turbine. At nozzle outlet the absolute Mach number at the nominal design point is

$$\mathrm{M}_2 = \frac{c_2}{a_2} = \frac{U_2}{a_2}\operatorname{cosec}\alpha_2.$$

Now,

$$T_2 = T_{01} - c_2^2/(2C_p) = T_{01} - \frac{1}{2}U_2^2\operatorname{cosec}^2\alpha_2/C_p.$$

Therefore,

$$\frac{T_2}{T_{01}} = 1 - \frac{1}{2}(\gamma-1)(U_2/a_{01})^2\operatorname{cosec}^2\alpha_2,$$

where $a_2 = a_{01}(T_2/T_{01})^{1/2}$. Hence,

$$\mathrm{M}_2 = \frac{U_2/a_{01}}{\sin\alpha_2\left[1 - \frac{1}{2}(\gamma-1)(U_2/a_{01})^2\operatorname{cosec}^2\alpha_2\right]^{1/2}}. \tag{8.14}$$

At rotor outlet the relative Mach number at the design point is defined by

$$\mathrm{M}_{3,\mathrm{rel}} = \frac{w_3}{a_3} = \frac{r_3U_2}{r_2a_3}\operatorname{cosec}\beta_3.$$

Now,

$$h_3 = h_{01} - \left(U_2^2 + \frac{1}{2}c_3^2\right) = h_{01} - \left(U_2^2 + \frac{1}{2}U_3^2\cot^2\beta_3\right) = h_{01} - U_2^2\left[1 + \frac{1}{2}\left(\frac{r_3}{r_2}\cot\beta_3\right)^2\right],$$

$$a_3^2 = a_{01}^2 - (\gamma-1)U_2^2\left[1 + \frac{1}{2}\left(\frac{r_3}{r_2}\cot\beta_3\right)^2\right];$$

therefore,

$$\mathrm{M}_{3,\mathrm{rel}} = \frac{(U_2/a_{01})(r_3/r_2)}{\sin\beta_3\left\{1 - (\gamma-1)(U_2/a_{01})^2\left[1 + \frac{1}{2}\left(\frac{r_3}{r_2}\cot\beta_3\right)^2\right]\right\}^{1/2}}. \tag{8.15}$$

8.7 LOSS COEFFICIENTS IN 90° IFR TURBINES

There are a number of ways of representing the losses in the passages of 90° IFR turbines and these have been listed and inter-related by Benson (1970). As well as the nozzle and rotor passage losses there is a loss at rotor entry at off-design conditions. This occurs when the relative flow entering

the rotor is at some angle of incidence to the radial vanes so that it can be called an *incidence loss*. It is often referred to as *shock loss* but this can be a rather misleading term because, usually, there is no shock wave.

Nozzle Loss Coefficients

The enthalpy loss coefficient, which normally includes the inlet scroll losses, has already been defined and is

$$\zeta_N = (h_2 - h_{2s})/\left(\frac{1}{2}c_2^2\right). \tag{8.16}$$

Also in use is the isentropic velocity coefficient,

$$\phi_N = c_2/c_{2s}, \tag{8.17}$$

and the stagnation pressure loss coefficient,

$$Y_N = (p_{01} - p_{02})/(p_{02} - p_2), \tag{8.18a}$$

which can be related, approximately, to ζ_N by

$$Y_N \simeq \zeta_N\left(1 + \frac{1}{2}\gamma \mathrm{M}_2^2\right). \tag{8.18b}$$

Since $h_{01} = h_2 + \frac{1}{2}c_2^2 = h_{2s} + \frac{1}{2}c_{2s}^2$, $h_2 - h_{2s} = \frac{1}{2}\left(c_{2s}^2 - c_2^2\right)$ and

$$\zeta_N = \frac{1}{\phi_N^2} - 1. \tag{8.19}$$

Practical values of ϕ_N for well-designed nozzle rows in normal operation are usually in the range $0.90 < \phi_N < 0.97$ and $0.23 < \zeta_N < 0.063$.

Rotor Loss Coefficients

At either the design condition (Figure 8.4), or at the off-design condition dealt with later (Figure 8.5), the rotor passage friction losses can be expressed in terms of the following coefficients.

The enthalpy loss coefficient is

$$\zeta_R = (h_3 - h_{3s})/\left(\frac{1}{2}w_3^2\right). \tag{8.20}$$

The velocity coefficient is

$$\phi_R = w_3/w_{3s}, \tag{8.21}$$

which is related to ζ_R by

$$\zeta_R = \frac{1}{\phi_R^2} - 1. \tag{8.22}$$

The normal range of ϕ for well-designed rotors is approximately, $0.70 < \phi_R < 0.85$ and $1.04 < \zeta_R < 0.38$.

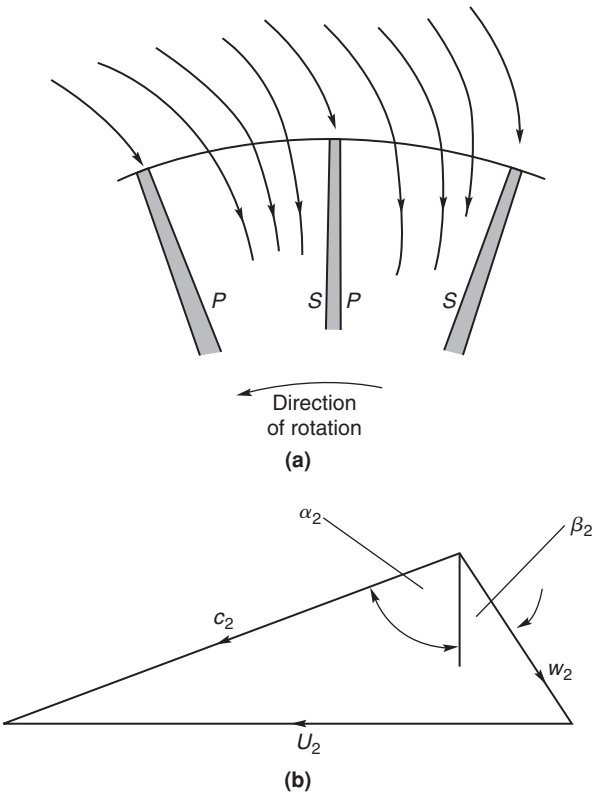

FIGURE 8.5

Optimum Flow Condition at Inlet to the Rotor: (a) Streamline Flow at Rotor Inlet—*p* is for Pressure Surface, *s* is for Suction Surface; (b) Velocity Diagram for the Pitchwise Averaged Flow

8.8 OPTIMUM EFFICIENCY CONSIDERATIONS

According to Abidat et al. (1992) the understanding of incidence effects on the rotors of radial- and mixed-flow turbines is very limited. Normally, IFR turbines are made with radial vanes to reduce bending stresses. In most flow analyses that have been published of the IFR turbine, including all earlier editions of this text, it was assumed that the *average* relative flow at entry to the rotor was radial, i.e., the incidence of the relative flow approaching the radial vanes was zero. The following discussion of the flow model will show that this is an over-simplification and the flow angle for optimum efficiency is significantly different from zero incidence. Rohlik (1975) had asserted that "there is some incidence angle that provides *optimum flow conditions* at the rotor-blade leading edge. This angle has a value sometimes as high as 40° with a radial blade."

The flow approaching the rotor is assumed to be in the radial plane with a velocity c_2 and flow angle α_2 determined by the geometry of the nozzles or volute. Once the fluid enters the rotor the

process of work extraction proceeds rapidly with reduction in the magnitude of the tangential velocity component and blade speed as the flow radius decreases. Corresponding to these velocity changes is a high blade loading and an accompanying large pressure gradient across the passage from the pressure side to the suction side [Figure 8.5(a)].

With the rotor rotating at angular velocity Ω and the entering flow assumed to be irrotational, a counter-rotating vortex (or relative eddy) is created in the relative flow, whose magnitude is $-\Omega$, which conserves the irrotational state. The effect is virtually the same as that described earlier for the flow leaving the impeller of a centrifugal compressor but in reverse (see Section 7.8 entitled "Slip Factor"). As a result of combining the incoming irrotational flow with the relative eddy, the relative velocity on the pressure (or trailing) surface of the vane is reduced. Similarly, on the suction (or leading) surface of the vane it is seen that the relative velocity is increased. Thus, a static pressure gradient exists *across* the vane passage in agreement with the reasoning of the preceding paragraph.

Figure 8.5(b) indicates the *average* relative velocity w_2, entering the rotor at angle β_2 and giving optimum flow conditions at the vane leading edge. As the rotor vanes in IFR turbines are assumed to be radial, the angle β_2 is an angle of incidence, and as drawn it is numerically positive. Depending upon the number of rotor vanes this angle may be between 20° and 40°. The static pressure gradient across the passage causes a streamline shift of the flow towards the suction surface. Stream function analyses of this flow condition show that the streamline pattern properly locates the inlet stagnation point on the vane leading edge so that this streamline is approximately radial [see Figure 8.5(a)]. It is reasoned that only at this flow condition will the fluid move smoothly into the rotor passage. Thus, it is the *averaged* relative flow that is at an angle of incidence β_2 to the vane. Whitfield and Baines (1990) have comprehensively reviewed computational methods used in determining turbomachinery flows, including stream function methods.

Wilson and Jansen (1965) appear to have been the first to note that the optimum angle of incidence was virtually identical to the angle of "slip" of the flow leaving the impeller of a radially bladed centrifugal compressor with the same number of vanes as the turbine rotor. Following Whitfield and Baines (1990), an *incidence factor*, λ, is defined, analogous to the slip factor used in centrifugal compressors:

$$\lambda = c_{\theta 2}/U_2.$$

The slip factor most often used in determining the flow angle at rotor inlet is that devised by Stanitz (1952) for radial vaned impellers, so for the incidence factor

$$\lambda = 1 - 0.63\pi/Z \approx 1 - 2/Z. \tag{7.34b}$$

Thus, from the geometry of Figure 8.5(b), we obtain

$$\tan\beta_2 = (2/Z)U_2/c_{m2}. \tag{8.23}$$

To determine the relative flow angle, β_2, we need to know, at least, the values of the flow coefficient, $\phi_2 = c_{m2}/U_2$ and the vane number Z. A simple method of determining the minimum number of vanes needed in the rotor, due to Jamieson (1955), is given later in this chapter. However, in the next section an optimum efficiency design method devised by Whitfield (1990) provides an alternative way for deriving β_2.

Design for Optimum Efficiency

Whitfield (1990) presented a general one-dimensional design procedure for the IFR turbine in which, initially, only the required power output is specified. The specific power output is given:

$$\Delta W = \frac{\dot{W}}{\dot{m}} = h_{01} - h_{03} = \frac{\gamma R}{\gamma - 1}(T_{01} - T_{03}) \tag{8.24}$$

and, from this a non-dimensional *power ratio*, S, is defined:

$$S = \Delta W / h_{01} = 1 - T_{03}/T_{01}. \tag{8.25}$$

The power ratio is related to the overall pressure ratio through the total-to-static efficiency:

$$\eta_{ts} = \frac{S}{\left[1 - (p_3/p_{01})^{(\gamma-1)/\gamma}\right]}. \tag{8.26}$$

If the power output, mass flow rate, and inlet stagnation temperature are specified, then S can be directly calculated but, if only the output power is known, then an iterative procedure must be followed.

Whitfield (1990) chose to develop his procedure in terms of the power ratio S and evolved a new non-dimensional design method. At a later stage of the design when the rate of mass flow and inlet stagnation temperature can be quantified, the actual gas velocities and turbine size can be determined. Only the first part of Whitfield's method dealing with the rotor design is considered in this chapter.

Solution of Whitfield's Design Problem

At the design point it is usually assumed that the fluid discharges from the rotor in the axial direction so that with $c_{\theta 3} = 0$, the specific work is

$$\Delta W = U_2 c_{\theta 2}$$

and, combining this with eqns. (8.24) and (8.25), we obtain

$$U_2 c_{\theta 2}/a_{01}^2 = S/(\gamma - 1), \tag{8.27}$$

where $a_{01} = (\gamma R T_{01})^{1/2}$ is the speed of sound corresponding to the temperature T_{01}.

Now, from the velocity triangle at rotor inlet, Figure 8.5(b),

$$U_2 - c_{\theta 2} = c_{m2} \tan\beta_2 = c_{\theta 2} \tan\beta_2 / \tan\alpha_2. \tag{8.28}$$

Multiplying both sides of eqn. (8.28) by $c_{\theta 2}/c_{m2}^2$, we get

$$U_2 c_{\theta 2}/c_{m2}^2 - c_{\theta 2}^2/c_{m2}^2 - \tan\alpha_2 \tan\beta_2 = 0.$$

But,

$$U_2 c_{\theta 2}/c_{m2}^2 = (U_2 c_{\theta 2}/c_2^2)\sec^2\alpha_2 = c(1 + \tan^2\alpha_2),$$

which can be written as a quadratic equation for $\tan\alpha_2$:

$$(c-1)\tan^2\alpha_2 - b\tan\alpha_2 + c = 0,$$

where, for economy of writing, $c = U_2 c_{\theta 2}/c_2^2$ and $b = \tan\beta_2$. Solving for $\tan\alpha_2$,

$$\tan\alpha_2 = \left[b \pm \sqrt{b^2 + 4c(1-c)}\right]/2(c-1). \tag{8.29}$$

For a real solution to exist the radical must be greater than, or equal to, zero; i.e., $b^2 + 4c(1-c) \geq 0$. Taking the zero case and rearranging the terms, another quadratic equation is found, namely,

$$c^2 - c - b^2/4 = 0.$$

Hence, solving for c,

$$c = \left(1 \pm \sqrt{1+b^2}\right)/2 = \frac{1}{2}(1 \pm \sec\beta_2) = U_2 c_{\theta 2}/c_2^2. \tag{8.30}$$

From eqn. (8.29) and then eqn. (8.30), the corresponding solution for $\tan\alpha_2$ is

$$\tan\alpha_2 = b/[2(c-1)] = \tan\beta_2/(-1 \pm \sec\beta_2).$$

The correct choice between these two solutions will give a value for $\alpha_2 > 0$; thus

$$\tan\alpha_2 = \frac{\sin\beta_2}{1-\cos\beta_2}. \tag{8.31a}$$

It is easy to see from Table 8.1 that a simple numerical relation exists between these two parameters, namely,

$$\alpha_2 = 90 - \beta_2/2. \tag{8.31b}$$

From eqns. (8.27) and (8.30), after some rearranging, a minimum stagnation Mach number at rotor inlet can be found:

$$\mathrm{M}_{02}^2 = c_2^2/a_{01}^2 = \left(\frac{S}{\gamma - 1}\right)\frac{2\cos\beta_2}{1+\cos\beta_2} \tag{8.32}$$

and the inlet Mach number can be determined using the equation

$$\mathrm{M}_2^2 = \left(\frac{c_2}{a_2}\right)^2 = \frac{\mathrm{M}_{02}^2}{1 - \frac{1}{2}(\gamma-1)\mathrm{M}_{02}^2}, \tag{8.33}$$

assuming that $T_{02} = T_{01}$, as the flow through the stator is adiabatic.

Now, from eqn. (8.28)

$$\frac{c_{\theta 2}}{U_2} = \frac{1}{1 + \tan\beta_2/\tan\alpha_2}.$$

Table 8.1 Variation of α_2 for Several Values of β_2

	Degrees			
$\beta 2$	10	20	30	40
$\alpha 2$	85	80	75	70

After rearranging eqn. (8.31a) to give

$$\tan\beta_2/\tan\alpha_2 = \sec\beta_2 - 1 \tag{8.34}$$

and, combining these equations with eqn. (8.23),

$$c_{\theta 2}/U_2 = \cos\beta_2 = 1 - 2/Z. \tag{8.35}$$

Equation (8.35) is a direct relationship between the number of rotor blades and the relative flow angle at inlet to the rotor. Also, from eqn. (8.31b),

$$\cos 2\alpha_2 = \cos(180 - \beta_2) = -\cos\beta_2,$$

so that, from the identity $\cos 2\alpha_2 = 2\cos^2\alpha_2 - 1$, we get the result

$$\cos^2\alpha_2 = (1 - \cos\beta_2)/2 = 1/Z, \tag{8.31c}$$

using also eqn. (8.35).

Example 8.3

An IFR turbine with 12 vanes is required to develop 230 kW from a supply of dry air available at a stagnation temperature of 1050 K and a flow rate of 1 kg/s. Using the optimum efficiency design method and assuming a total-to-static efficiency of 0.81, determine

(i) the absolute and relative flow angles at rotor inlet;
(ii) the overall pressure ratio, p_{01}/p_3;
(iii) the rotor tip speed and the inlet absolute Mach number.

Solution

(i) From the gas tables, e.g., Rogers and Mayhew (1995) or NIST Properties of Fluids Tables, at $T_{01} = 1050$ K, we can find values for $C_p = 1.1502$ kJ/kgK and $\gamma = 1.333$. Using eqn. (8.25),

$$S = \Delta W/(C_p T_{01}) = 230/(1.15 \times 1050) = 0.2.$$

From Whitfield's eqn. (8.31c),

$$\cos^2\alpha_2 = 1/Z = 0.083333,$$

therefore, $\alpha_2 = 73.22°$ and, from eqn. (8.31b), $\beta_2 = 2(90 - \alpha_2) = 33.56°$.

(ii) Rewriting eqn. (8.26),

$$\frac{p_3}{p_{01}} = \left(1 - \frac{S}{\eta_{ts}}\right)^{\gamma/(\gamma-1)} = \left(1 - \frac{0.2}{0.81}\right)^4 = 0.32165,$$

therefore, $p_{01}/p_{003} = 3.109$.

(iii) Using eqn. (8.32),

$$\mathrm{M}_{02}^2 = \left(\frac{\mathrm{S}}{\gamma - 1}\right)\frac{2\cos\beta_2}{1 + \cos\beta_2} = \frac{0.2}{0.333} \times \frac{2 \times 0.8333}{1 + 0.8333} = 0.5460$$

therefore, M = 0.7389. Using eqn. (8.33),

$$M_2^2 = \frac{M_{02}^2}{1 - \frac{1}{2}(\gamma - 1)M_{02}^2} = \frac{0.546}{1 - (0.333/2) \times 0.546} = 0.6006$$

and $M_2 = 0.775$. To find the rotor tip speed, substitute eqn. (8.35) into eqn. (8.27) to obtain

$$\left(\frac{U_2^2}{a_{01}^2}\right) \cos\beta_2 = \frac{S}{\gamma - 1},$$

therefore,

$$U_2 = a_{01}\sqrt{\frac{S}{(\gamma - 1)\cos\beta_2}} = 633.8\sqrt{\frac{0.2}{0.333 \times 0.8333}} = 538.1\ \text{m/s},$$

where

$$a_{01} = \sqrt{\gamma R T_{01}} = \sqrt{1.333 \times 287 \times 1,050} = 633.8\ \text{m/s},$$

and $T_{02} = T_{01}$ is assumed.

8.9 CRITERION FOR MINIMUM NUMBER OF BLADES

The following simple analysis of the relative flow in a radially bladed rotor is of considerable interest as it illustrates an important fundamental point concerning blade spacing. From elementary mechanics, the radial and transverse components of acceleration, f_r and f_t, respectively, of a particle moving in a radial plane [Figure 8.6(a)] are

$$f_r = \dot{w} - \Omega^2 r \tag{8.36a}$$

$$f_t = r\dot{\Omega} + 2\Omega w, \tag{8.36b}$$

where w is the radial velocity, $\dot{w} = (\mathrm{d}w)/(\mathrm{d}t) = w(\partial w)/(\partial r)$ (for steady flow), Ω is the angular velocity and $\dot{\Omega} = \mathrm{d}\Omega/\mathrm{d}t$ is set equal to zero.

Applying *Newton's second law of motion* to a fluid element (as shown in Figure 6.2) of unit depth, ignoring viscous forces, but putting $c_r = w$, the radial equation of motion is

$$(p + \mathrm{d}p)(r + \mathrm{d}r)\mathrm{d}\theta - pr\mathrm{d}\theta - p\mathrm{d}r\mathrm{d}\theta = -f_r \mathrm{d}m,$$

where the elementary mass $\mathrm{d}m = \rho r \mathrm{d}\theta \mathrm{d}r$. After simplifying and substituting for f_r from eqn. (8.36a), the following result is obtained,

$$\frac{1}{\rho}\frac{\partial p}{\partial r} + w\frac{\partial w}{\partial r} = \Omega^2 r. \tag{8.37}$$

Integrating eqn. (8.37) with respect to r obtains

$$p/\rho + \frac{1}{2}w^2 - \frac{1}{2}U^2 = \text{constant}, \tag{8.38}$$

which is merely the *inviscid form* of eqn. (8.2a).

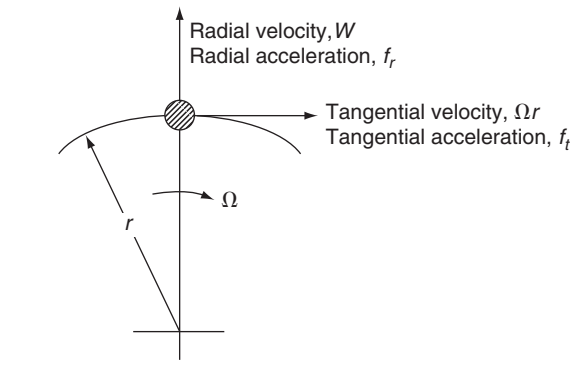

(a) Motion of particle in a radial plane

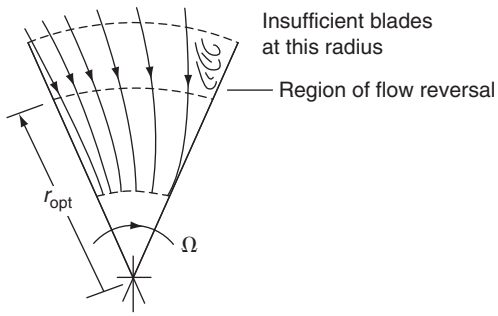

(b) Optimum radius to avoid flow reversal, r_{opt}

FIGURE 8.6

Flow Models Used in Analysis of Minimum Number of Blades

The torque transmitted to the rotor by the fluid manifests itself as a pressure difference across each radial vane. Consequently, there must be a pressure gradient in the *tangential direction* in the space between the vanes. Again, consider the element of fluid and apply Newton's second law of motion in the tangential direction:

$$\mathrm{d}p \times \mathrm{d}r = f_t \mathrm{d}m = 2\Omega w(\rho r \mathrm{d}\theta \mathrm{d}r).$$

Hence,

$$\frac{1}{\rho}\frac{\partial p}{\partial \theta} = 2\Omega r w, \tag{8.39}$$

which establishes the magnitude of the tangential pressure gradient. Differentiating eqn. (8.38) with respect to θ,

$$\frac{1}{\rho}\frac{\partial p}{\partial \theta} = -w\frac{\partial w}{\partial \theta}. \tag{8.40}$$

Thus, combining eqns. (8.39) and (8.40) gives

$$\frac{\partial w}{\partial \theta} = -2\Omega r. \tag{8.41}$$

This result establishes the important fact that *the radial velocity is not uniform across the passage* as is frequently assumed. As a consequence the radial velocity on one side of a passage is lower than on the other side. Jamieson (1955), who originated this method, conceived the idea of determining the *minimum* number of blades based upon these velocity considerations.

Let the mean radial velocity be $\overline{w}$ and the angular space between two adjacent blades be $\Delta\theta = 2\pi/Z$ where Z is the number of blades. The maximum and minimum radial velocities are, therefore,

$$w_{\max} = \overline{w} + \frac{1}{2}\Delta w = \overline{w} + \Omega r \Delta\theta \tag{8.42a}$$

$$w_{\min} = \overline{w} - \frac{1}{2}\Delta w = \overline{w} - \Omega r \Delta\theta \tag{8.42b}$$

using eqn. (8.41).

Making the reasonable assumption that the radial velocity should not drop below zero [see Figure 8.6(b)], the limiting case occurs at the rotor tip, $r = r_2$ with $w_{\min} = 0$. From eqn. (8.42b) with $U_2 = \Omega r_2$, the minimum number of rotor blades is

$$Z_{\min} = 2\pi U_2/\overline{w}_2. \tag{8.43a}$$

At the design condition, $U_2 = \overline{w}_2 \tan\alpha_2$, hence,

$$Z_{\min} = 2\pi \tan\alpha_2. \tag{8.43b}$$

Jamieson's result, eqn. (8.43b), is plotted in Figure 8.7 and shows that a large number of rotor vanes are required, especially for high absolute flow angles at rotor inlet. In practice a large number of vanes are not used for several reasons, e.g., excessive flow blockage at rotor exit, a disproportionally large "wetted" surface area causing high friction losses, and the weight and inertia of the rotor become relatively high.

Some experimental tests reported by Hiett and Johnston (1964) are of interest in connection with the analysis just presented. With a nozzle outlet angle $\alpha_2 = 77°$ and a 12 vane rotor, a total-to-static efficiency $\eta_{ts} = 0.84$ was measured at the optimum velocity ratio U_2/c_0. For that magnitude of flow angle, eqn. (8.43b) suggests 27 vanes would be required to avoid reverse flow at the rotor tip. However, a second test with the number of vanes increased to 24 produced a gain in efficiency of only 1%. Hiett and Johnston suggested that the criterion for the optimum number of vanes might not simply be the avoidance of local flow reversal but require a compromise between total pressure losses from this cause and friction losses based upon rotor and blade surface areas.

Glassman (1976) preferred to use an empirical relationship between Z and α_2, namely,

$$Z = \frac{\pi}{30}(110 - \alpha_2)\tan\alpha_2, \tag{8.44}$$

as he also considered Jamieson's result, eqn. (8.43b), gave too many vanes in the rotor. Glassman's result, which gives far fewer vanes than Jamieson's is plotted in Figure 8.7. Whitfield's result, given in eqn. (8.31c), is not too dissimilar from the result given by Glassman's equation, at least for low vane numbers.

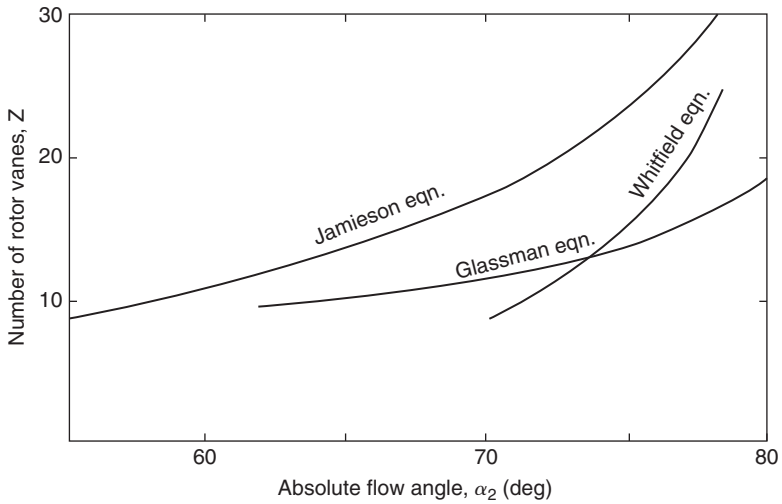

FIGURE 8.7

Flow Angle at Rotor Inlet as a Function of the Number of Rotor Vanes

8.10 DESIGN CONSIDERATIONS FOR ROTOR EXIT

Several decisions need to be made regarding the design of the rotor exit. The flow angle β_3, the meridional velocity to blade tip speed ratio c_{m3}/U_2, the shroud tip to rotor tip radius ratio r_{3s}/r_2, and the exit hub to shroud radius ratio $v = r_{3h}/r_{3s}$, all have to be considered. It is assumed that the absolute flow at rotor exit is entirely axial so that the relative velocity can be written

$$w_3^2 = c_{m3}^2 + U_3^2.$$

If values of c_{m3}/U_2 and r_3/r_2 can be chosen, then the exit flow angle variation can be found for all radii. From the rotor exit velocity diagram in Figure 8.3,

$$\cot\beta_3(r) = \frac{c_{m3}}{U_2}\frac{r_2}{r} \tag{8.45}$$

The meridional velocity c_{m3} should be kept small in order to minimise the exhaust energy loss, unless an exhaust diffuser is fitted to the turbine.

Rodgers and Geiser (1987) correlated attainable efficiency levels of IFR turbines against the blade tip speed–spouting velocity ratio, U_2/c_0, and the axial exit flow coefficient, c_{m3}/U_2, and their result is shown in Figure 8.8. From this figure it can be seen that peak efficiency values are obtained with velocity ratios close to 0.7 and with values of exit flow coefficient between 0.2 and 0.3.

Rohlik (1968) suggested that the ratio of mean rotor exit radius to rotor inlet radius, r_3/r_2, should not exceed 0.7 to avoid excessive curvature of the shroud. Also, the exit hub to shroud radius

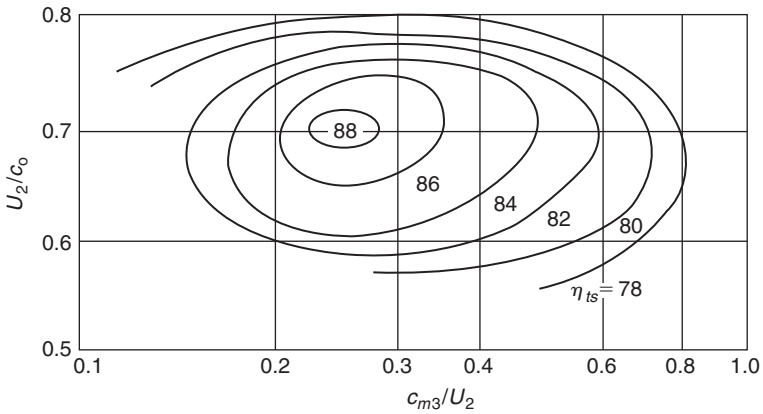

FIGURE 8.8

Correlation of Attainable Efficiency Levels of IFR Turbines against Velocity Ratios (Adapted from Rodgers and Geiser, 1987)

ratio, r_{3h}/r_{3s}, should not be less than 0.4 because of the likelihood of flow blockage caused by closely spaced vanes. Based upon the metal thickness alone it is easily shown that

$$(2\pi r_3 h/Z)\cos\beta_{3h} > t_{3h},$$

where t_{3h} is the vane thickness at the hub. It is also necessary to allow more than this thickness because of the boundary layers on each vane. Some of the rather limited test data available on the design of the rotor exit comes from Rodgers and Geiser (1987) and concerns the effect of rotor radius ratio and blade solidity on turbine efficiency (see Figure 8.9). It is the relative efficiency variation, η/η_{opt}, that is depicted as a function of the rotor inlet radius–exit *root mean square* radius ratio, $r_2/r_{3\text{rms}}$, for various values of a blade solidity parameter, ZL/D_2 (where L is the length of the blade along the mean meridian). This radius ratio is related to the rotor exit hub to shroud ratio, v, by

$$\frac{r_{3\text{rms}}}{r_2} = \frac{r_{3s}}{r_2}\left(\frac{1+v^2}{2}\right)^{1/2}.$$

From Figure 8.9, for $r_2/r_{3\text{rms}}$, a value between 1.6 and 1.8 appears to be the optimum.

Rohlik (1968) suggested that the ratio of the relative velocity at the mean exit radius to the inlet relative velocity, w_3/w_2, should be sufficiently high to assure a low total pressure loss. He gave w_3/w_2 a value of 2.0. The relative velocity at the shroud tip will be greater than that at the mean radius depending upon the radius ratio at rotor exit.

Example 8.4

Given the following data for an IFR turbine,

$$c_{m3}/U_2 = 0.25,\ v = 0.4,\ r_{3s}/r_2 = 0.7 \quad \text{and} \quad w_3/w_2 = 2.0,$$

determine the ratio of the relative velocity ratio, w_{3s}/w_2 at the shroud.

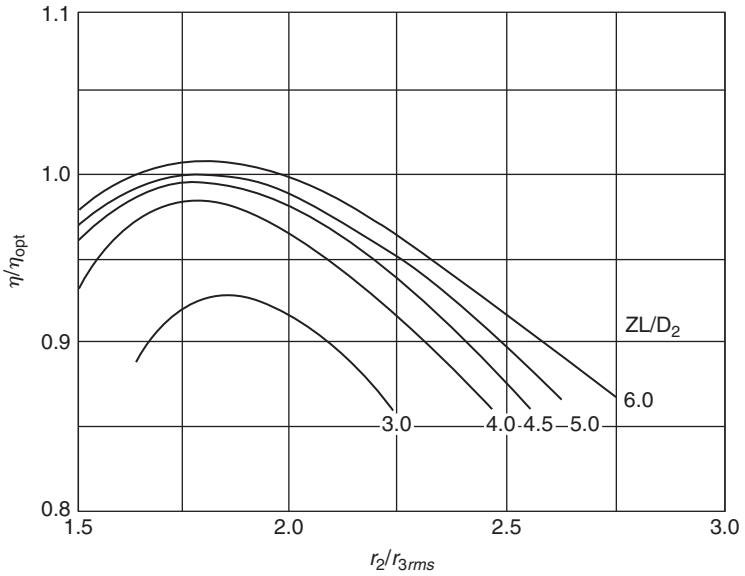

FIGURE 8.9

Effects of Vane Solidity and Rotor Radius Ratio on the Efficiency Ratio of the IFR Turbine (Adapted from Rodgers and Geiser, 1987)

Solution

As $w_{3s}/c_{m3} = \sec\beta_{3s}$ and $w_3/c_{m3} = \sec\beta_3$,

$$\frac{w_{3s}}{w_3} = \frac{\sec\beta_{3s}}{\sec\beta_3}.$$

$$\frac{r_3}{r_{3s}} = \frac{1}{2}(1+v) = 0.7 \quad \text{and} \quad \frac{r_3}{r_2} = \frac{r_3}{r_{3s}}\frac{r_{3s}}{r_2} = 0.7 \times 0.7 = 0.49.$$

From eqn. (8.45), the angle at mean radius is given by,

$$\cot\beta_3 = \frac{c_{m3}}{U_2}\frac{r_2}{r_3} = \frac{0.25}{0.49} = 0.5102$$

hence, $\beta_3 = 62.97°$,

$$\cot\beta_{3s} = \frac{c_{m3}}{U_2}\frac{r_2}{r_{3s}} = \frac{0.25}{0.7} = 0.3571$$

hence, $\beta_{3s} = 70.35°$, and, therefore,

$$\frac{w_{3s}}{w_2} = \frac{w_{3s}}{w_3}\frac{w_3}{w_2} = \frac{\sec\beta_{3s}}{\sec\beta_3} \times 2 = \frac{0.4544}{0.3363} \times 2 = 2.702.$$

The relative velocity ratio will increase progressively from the hub to the shroud.

Example 8.5

Using the data and results given in Examples 8.3 and 8.4 together with the additional information that the static pressure at rotor exit is 100 kPa and the nozzle enthalpy loss coefficient, $\zeta_N = 0.06$, determine

(i) the diameter of the rotor and its speed of rotation;
(ii) the vane width to diameter ratio, b_2/D_2 at rotor inlet.

Solution

(i) The rate of mass flow is given by

$$\dot{m} = \rho_3 c_{m3} A_3 = \left(\frac{p_3}{RT_3}\right)\left(\frac{c_{m3}}{U_2}\right) U_2 \pi \left(\frac{r_{3s}}{r_2}\right)^2 (1 - \nu^2) r_2^2.$$

From eqn. (8.25), $T_{03} = T_{01}(1 - S) = 1050 \times 0.8 = 840\,\text{K}$,

$$T_3 = T_{03} - c_{m3}^2/(2C_p) = T_{03} - \left(\frac{c_{m3}}{U_2}\right)^2 \frac{U_2^2}{2C_p} = 840 - 0.25^2 \times 5.38.1^2/(2 \times 1150.2).$$

Hence, $T_3 = 832.1\,\text{K}$.
Substituting values into this mass flow equation,

$$1 = [10^5/(287 \times 832.1)] \times 0.25 \times 538.1 \times 0.7^2 \times \pi \times (1 - 0.4^2) r_2^2;$$

therefore,

$$r_2^2 = 0.01373 \quad \text{and} \quad r_2 = 0.1172\,\text{m},$$
$$D_2 = \underline{0.2343\,\text{m}}$$
$$\Omega = U_2/r_2 = 4591.3\,\text{rad/s}\ (N = \underline{43,843\,\text{rev/min}}).$$

(ii) The rate of mass flow equation is now written as

$$\dot{m} = \rho_2 c_{m2} A_2, \text{ where } A_2 = 2\pi r_2 b_2 = 4\pi r_2^2 (b_2/D_2).$$

Solving for the absolute velocity at rotor inlet and its components,

$$c_{\theta 2} = SC_p T_{01}/U_2 = 0.2 \times 1150.2 \times 1050/538.1 = 448.9\,\text{m/s},$$
$$c_{m2} = c_{\theta 2}/\tan\alpha_2 = 448.9/3.3163 = 135.4\,\text{m/s},$$
$$c_2 = c_{\theta 2}/\sin\alpha_2 = 448.9/0.9574 = 468.8\,\text{m/s}.$$

To obtain a value for the static density, ρ_2, we need to determine T_2 and p_2:

$$T_2 = T_{02} - c_2^2/(2C_p) = 1050 - 468.8^2/(2 \times 1150.2) = 954.5\,\text{K},$$

$$h_{02} - h_2 = \frac{1}{2}c_2^2 \text{ and as } \zeta_N = (h_2 - h_{2s})\Big/\left(\frac{1}{2}c_2^2\right), \quad h_{01} - h_{2s} = \frac{1}{2}c_2^2(1 + \zeta_N), \text{ so}$$

$$\frac{T_{02}-T_{2s}}{T_{02}}=\frac{c_2^2(1+\zeta_N)}{2C_pT_{02}}=\frac{468.8^2\times 1.06}{2\times 1150.2\times 1050}=0.096447$$

$$\frac{T_{2s}}{T_{01}}=\left(\frac{p_2}{p_{01}}\right)^{(\gamma-1)/\gamma}=1-0.09645=0.90355.$$

Therefore,

$$\frac{p_2}{p_{01}}=\left(\frac{T_{2s}}{T_{01}}\right)^{\gamma/(\gamma-1)}=0.90355^4=0.66652,$$

$$p_2=3.109\times 10^5\times 0.66652=2.0722\times 10^5\ \text{Pa},$$

$$\frac{b_2}{D_2}=\frac{1}{4\pi}\left(\frac{RT_2}{p_2}\right)\left(\frac{\dot{m}}{c_{m2}r_2^2}\right)=\frac{1}{4\times\pi}\left(\frac{287\times 954.5}{2.0722\times 10^5}\right)\frac{1}{135.4\times 0.01373}=\underline{0.0566.}$$

Example 8.6

For the IFR turbine described in Example 8.3 and using the data and results in Examples 8.4 and 8.5, deduce a value for the rotor enthalpy loss coefficient, ζ_R, at the optimum efficiency flow condition.

Solution

From eqn. (8.10), solving for ζ_R,

$$\zeta_R=[(1-\eta_{ts})c_0^2-c_3^2-\zeta_N c_2^2]/w_3^2.$$

We need to find values for c_0, c_3, w_3, and c_2.
From the data,

$$c_3=c_{m3}=0.25\times 538.1=134.5\,\text{m/s}.$$

$$w_3=2w_2=2c_{m2}/\cos\beta_2=2\times 135.4/\cos 33.560=324.97\,\text{m/s}.$$

$$\frac{1}{2}c_0^2=\Delta W/\eta_{ts}=230\times 10^3/0.81=283.95\times 10^3.$$

$$c_2=468.8\,\text{m/s}.$$

Therefore,

$$\zeta_R=(2\times 283.95\times 10^3\times 0.19-134.5^2-0.06\times 468.8^2)/324.97^2$$
$$=76,624/105,605=0.7256.$$

8.11 SIGNIFICANCE AND APPLICATION OF SPECIFIC SPEED

The concept of specific speed N_s has already been discussed in Chapter 2 and some applications of it have been made already. Specific speed is extensively used to describe turbomachinery operating requirements in terms of shaft speed, volume flow rate and ideal specific work (alternatively, power developed is used instead of specific work). Originally, specific speed was applied almost exclusively to *incompressible* flow machines as a tool in the selection of the optimum type and size of unit. Its application to units handling *compressible* fluids was somewhat inhibited, due, it would appear, to the fact that volume flow rate changes through the machine, which raised the awkward question of which flow rate should be used in the specific speed definition. According to Balje (1981), the significant volume flow rate that should be used for turbines is that in the rotor exit, Q_3. This has now been widely adopted by many authorities.

Wood (1963) found it useful to factorise the basic definition of the specific speed equation, eqn. (2.14a), in terms of the geometry and flow conditions within the radial-inflow turbine. Adopting the non-dimensional form of specific speed, to avoid ambiguities,

$$N_s = \frac{NQ_3^{1/2}}{\Delta h_{0s}^{3/4}}, \tag{8.46}$$

where N is in rev/s, Q_3 is in m^3/s, and the isentropic total-to-total enthalpy drop Δh_{0s} (from turbine inlet to exhaust) is in joules per kilogram (i.e., square metres per second squared).

For the 90° IFR turbine, writing $U_2 = \pi N D_2$ and $\Delta h_{0s} = \frac{1}{2}c_0^2$, eqn. (8.46) can be factorised as follows:

$$N_s = \frac{Q_3^{1/2}}{\left(\frac{1}{2}c_0^2\right)^{3/4}}\left(\frac{U_2}{\pi D_2}\right)\left(\frac{U_2}{\pi N D_2}\right)^{1/2} = \left(\frac{\sqrt{2}}{\pi}\right)^{3/2}\left(\frac{U_2}{c_0}\right)^{3/2}\left(\frac{Q_3}{ND_2^3}\right)^{1/2}. \tag{8.47a}$$

For the *ideal* 90° IFR turbine and with $c_{\theta 2} = U_2$, it was shown earlier that the blade speed to spouting velocity ratio, $U_2/c_0 = \sqrt{2} = 0.707$. Substituting this value into eqn. (8.47a),

$$N_s = 0.18\left(\frac{Q_3}{ND_2^3}\right)^{1/2}, \text{ (rev)} \tag{8.47b}$$

i.e., specific speed is directly proportional to the square root of the volumetric flow coefficient.

To obtain some physical significance from eqns. (8.46) and (8.47b), define a *rotor disc area* $A_d = \pi D_2^2/4$ and assume a uniform axial rotor exit velocity c_3 so that $Q_3 = A_3 c_3$, as

$$N = U_2/(\pi D_2) = \frac{c_0\sqrt{2}}{2\pi D_2}$$

$$\frac{Q_3}{ND_2^3} = \frac{A_3 c_3 2\pi D_2}{\sqrt{2}c_0 D_2^2} = \frac{A_3}{A_d}\frac{c_3}{c_0}\frac{\pi^2}{2\sqrt{2}}.$$

Hence,

$$N_s = 0.336\left(\frac{c_3}{c_0}\right)^{1/2}\left(\frac{A_3}{A_d}\right)^{1/2}, \text{ (rev)} \tag{8.47c}$$

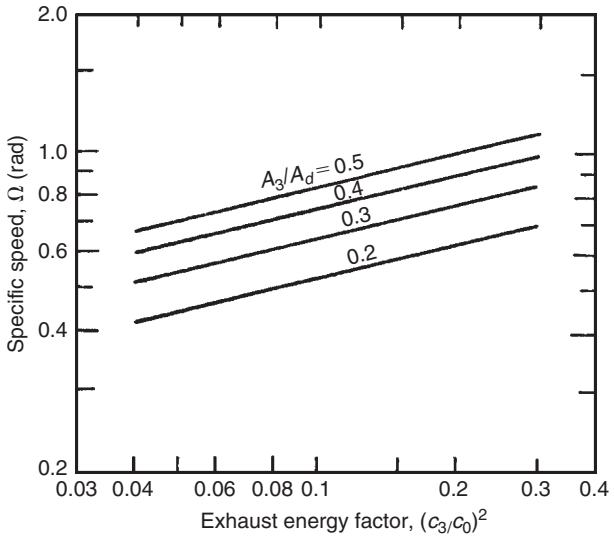

FIGURE 8.10

Specific Speed Function for a 90° Inward Flow Radial Turbine (Adapted from Wood, 1963)

or

$$\Omega_s = 2.11\left(\frac{c_3}{c_0}\right)^{1/2}\left(\frac{A_3}{A_d}\right)^{1/2}, \text{ (rad)} \tag{8.47d}$$

In an early study of IFR turbine design for maximum efficiency, Rohlik (1968) specified that the ratio of the rotor shroud diameter to rotor inlet diameter should be limited to a maximum value of 0.7 to avoid excessive shroud curvature and that the exit hub–shroud tip ratio was limited to a minimum of 0.4 to avoid excess hub blade blockage and loss. Using this as data, an upper limit for A_3/A_d can be found,

$$\frac{A_3}{A_d} = \left(\frac{D_{3s}}{D_2}\right)^2\left[1-\left(\frac{D_{3h}}{D_{3s}}\right)^2\right] = 0.7^2 \times (1-0.16) = 0.41.$$

Figure 8.10 shows the relationship between Ω_s, the exhaust energy factor $(c_3/c_0)^2$, and the area ratio A_3/A_d based upon eqn. (8.47d). According to Wood (1963), the limits for the exhaust energy factor in gas turbine practice are $0.04 < (c_3/c_0)^2 < 0.30$, the lower value being apparently a flow stability limit.

The numerical value of specific speed provides a general index of flow capacity relative to work output. Low values of Ω_s are associated with relatively small flow passage areas and high values with relatively large flow passage areas. Specific speed has also been widely used as a general indication of achievable efficiency. Figure 8.11 presents a broad correlation of maximum efficiencies for hydraulic and compressible fluid turbines as functions of specific speed. These efficiencies apply to

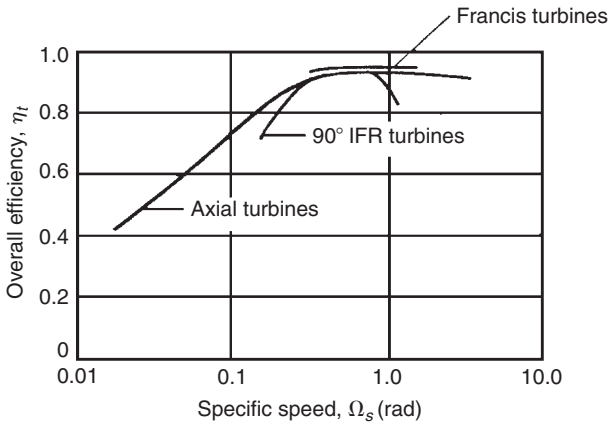

FIGURE 8.11

Specific Speed–Efficiency Characteristics for Various Turbines (Adapted from Wood, 1963)

favourable design conditions with high values of flow Reynolds number, efficient diffusers and low leakage losses at the blade tips. It is seen that over a limited range of specific speed the best radial-flow turbines match the best axial-flow turbine efficiency, but from $\Omega_s = 0.03$ to 10 no other form of turbine handling compressible fluids can exceed the peak performance capability of the axial turbine.

Over the fairly limited range of specific speed ($0.3 < \Omega_s < 1.0$) that the IFR turbine can produce a high efficiency, it is difficult to find a decisive performance advantage in favour of either the axial-flow turbine or the radial-flow turbine. New methods of fabrication enable the blades of small axial-flow turbines to be cast integrally with the rotor so that both types of turbine can operate at about the same blade tip speed. Wood (1963) compared the relative merits of axial and radial gas turbines at some length. In general, although weight, bulk, and diameter are greater for radial than axial turbines, the differences are not so large and mechanical design compatibility can reverse the difference in a complete gas turbine power plant. The NASA nuclear Brayton cycle space power studies were all made with 90° IFR turbines rather than with axial-flow turbines.

The design problems of a small axial-flow turbine were discussed by Dunham and Panton (1973) who studied the cold performance measurements made on a single-shaft turbine of 13 cm diameter, about the same size as the IFR turbines tested by NASA. Tests had been performed with four rotors to try to determine the effects of aspect ratio, trailing edge thickness, Reynolds number and tip clearance. One turbine build achieved a total-to-total efficiency of 90%, about equal to that of the best IFR turbine. However, because of the much higher outlet velocity, the total-to-static efficiency of the axial turbine gave a less satisfactory value (84%) than the IFR type which could be decisive in some applications. They also confirmed that the axial turbine tip clearance was comparatively large, losing 2% efficiency for every 1% increase in clearance. The tests illustrated one major design problem of a small axial turbine that was the extreme thinness of the blade trailing edges needed to achieve the efficiencies stated.

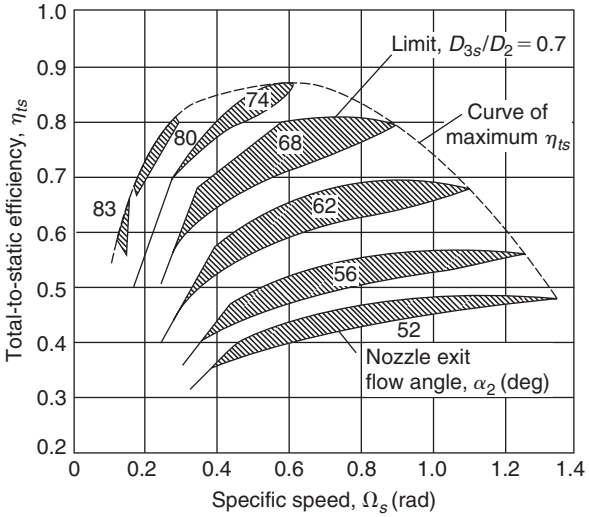

FIGURE 8.12

Calculated Performance of 90° IFR Turbine (Adapted from Rohlik, 1968)

8.12 OPTIMUM DESIGN SELECTION OF 90° IFR TURBINES

Rohlik (1968) has examined analytically the performance of 90° inward-flow radial turbines to determine *optimum* design geometry for various applications as characterised by specific speed. His procedure, which extends an earlier treatment of Wood (1963), was used to determine the design point losses and corresponding efficiencies for various combinations of nozzle exit flow angle α_2, rotor diameter ratio D_2/D_3, and rotor blade entry height to exit diameter ratio, b_2/D_3. The losses taken into account in the calculations are those associated with

(i) nozzle blade row boundary layers;
(ii) rotor passage boundary layers;
(iii) rotor blade tip clearance;
(iv) disc windage (on the back surface of the rotor);
(v) kinetic energy loss at exit.

A mean flow path analysis was used and the passage losses were based upon the data of Stewart, Witney, and Wong (1960). The main constraints in the analysis were

(i) $w_3/w_2 = 2.0$;
(ii) $c_{\theta 3} = 0$;
(iii) $\beta_2 = \beta_{2,\text{opt}}$, i.e., zero incidence;
(iv) $r_{3s}/r_2 = 0.7$;
(v) $r_{3h}/r_{3s} = 0.4$.

Figure 8.12 shows the variation in total-to-static efficiency with specific speed (Ω_s) for a selection of nozzle exit flow angles, α_2. For each value of α_2 a hatched area is drawn, inside of which the various

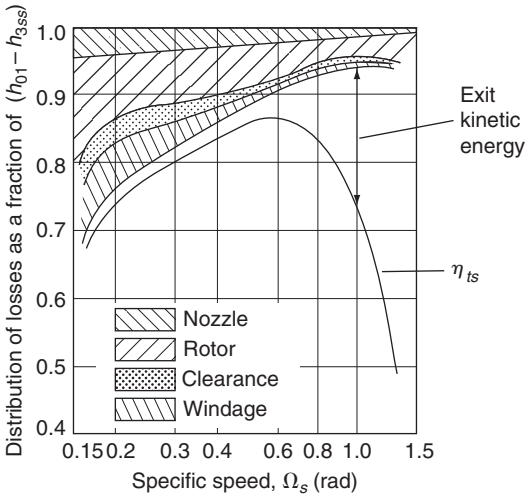

FIGURE 8.13

Distribution of Losses along Envelope of Maximum Total-to-Static Efficiency (Adapted from Rohlik, 1968)

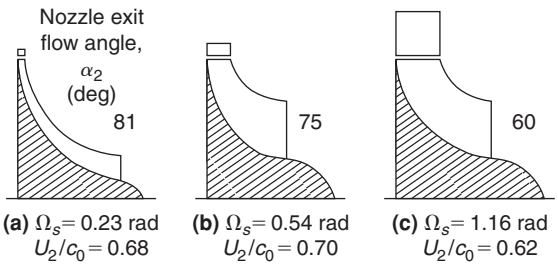

FIGURE 8.14

Sections of Radial Turbines of Maximum Static Efficiency (Adapted from Rohlik, 1968)

diameter ratios are varied. The envelope of maximum η_{ts} is bounded by the constraints $D_{3h}/D_{3s} = 0.4$ in all cases and $D_{3s}/D_2 = 0.7$ for $\Omega_s \geq 0.58$ in these hatched regions. This envelope is the *optimum geometry curve* and has a peak η_{ts} of 0.87 at $\Omega_s = 0.58$ rad. An interesting comparison is made by Rohlik with the experimental results obtained by Kofskey and Wasserbauer (1966) on a single 90° IFR turbine rotor operated with several nozzle blade row configurations. The peak value of η_{ts} from this experimental investigation also turned out to be 0.87 at a slightly higher specific speed, $\Omega_s = 0.64$ rad.

The distribution of losses for optimum geometry over the specific speed range is shown in Figure 8.13. The way the loss distributions change is a result of the changing ratio of flow to specific work. At low Ω_s all friction losses are relatively large because of the high ratios of surface area to flow area. At high Ω_s the high velocities at turbine exit cause the kinetic energy leaving loss to predominate.

Figure 8.14 shows several meridional plane sections at three values of specific speed corresponding to the curve of maximum total-to-static efficiency. The ratio of nozzle exit height–rotor diameter,

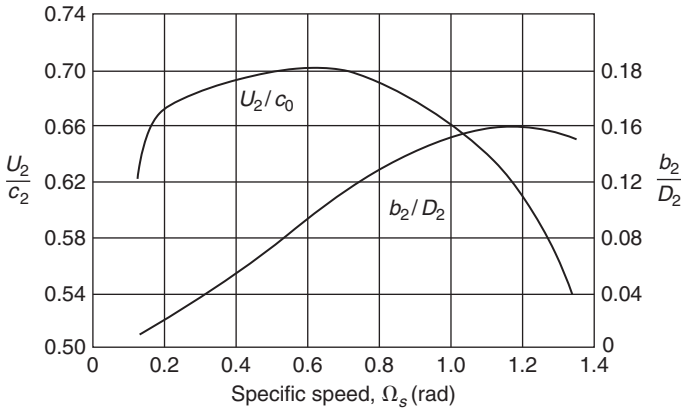

FIGURE 8.15

Variation in Blade Speed–Spouting Velocity Ratio (U_2/c_0) and Nozzle Blade Height–Rotor Inlet Diameter (b_2/D_2) Corresponding to Maximum Total-to-Static Efficiency with Specific Speed (Adapted from Rohlik, 1968)

b_2/D_2, is shown in Figure 8.15, the general rise of this ratio with increasing Ω_s reflecting the increase in nozzle flow area[3] accompanying the larger flow rates of higher specific speed. Figure 8.15 also shows the variation of U_2/c_0 with Ω_s along the curve of maximum total-to-static efficiency.

8.13 CLEARANCE AND WINDAGE LOSSES

A clearance gap must exist between the rotor vanes and the shroud. Because of the pressure difference between the pressure and suction surfaces of a vane, a leakage flow occurs through the gap introducing a loss in efficiency of the turbine. The minimum clearance is usually a compromise between manufacturing difficulty and aerodynamic requirements. Often, the minimum clearance is determined by the differential expansion and cooling of components under *transient* operating conditions that can compromise the steady state operating condition. According to Rohlik (1968) the loss in specific work as a result of gap leakage can be determined with the simple proportionality

$$\Delta h_c = \Delta h_0 (c/b_m), \tag{8.48}$$

where Δh_0 is the turbine specific work uncorrected for clearance or windage losses and c/b_m is the ratio of the gap to average vane height [i.e., $b_m = \frac{1}{2}(b_2 + b_3)$]. A constant axial and radial gap, $c = 0.25$ mm, was used in the analytical study of Rohlik quoted earlier. According to Rodgers (1969) extensive development on small gas turbines has shown that it is difficult to maintain clearances less than about 0.4 mm. One consequence of this is that as small gas turbines are made progressively smaller the *relative* magnitude of the clearance loss must increase.

[3]The ratio b_2/D_2 is also affected by the pressure ratio but this has not been shown.

The non-dimensional power loss due to windage on the back of the rotor has been given by Shepherd (1956) in the form

$$\Delta P_w/(\rho_2 \Omega^3 D_2^5) = \text{constant} \times \text{Re}^{-1/5},$$

where Ω is the rotational speed of the rotor and Re is a Reynolds number. Rohlik (1968) used this expression to calculate the loss in specific work due to windage,

$$\Delta h_w = 0.56\, \rho_2 D_2^2 (U_2/100)^3/(\dot{m}\ \text{Re}), \tag{8.49}$$

where $\dot{m}$ is the total rate of mass flow entering the turbine and the Reynolds number is defined by $\text{Re} = U_2 D_2/\nu_2$, ν_2 being the kinematic viscosity of the gas corresponding to the static temperature T_2 at nozzle exit.

8.14 COOLED 90° IFR TURBINES

The incentive to use higher temperatures in the basic Brayton gas turbine cycle is well known and arises from a desire to increase cycle efficiency and specific work output. In all gas turbines designed for high efficiency a compromise is necessary between the turbine inlet temperature desired and the temperature that can be tolerated by the turbine materials used. This problem can be minimised by using an auxiliary supply of cooling air to lower the temperature of the highly stressed parts of the turbine exposed to the high temperature gas. Following the successful application of blade cooling techniques to axial flow turbines, methods of cooling small radial gas turbines have been developed.

According to Rodgers (1969) the most practical method of cooling small radial turbines is by film (or veil) cooling, Figure 8.16, where cooling air is impinged on the rotor and vane tips. The main problem with this method of cooling being its relatively low *cooling effectiveness*, defined by

$$\varepsilon = \frac{T_{01} - (T_m + \Delta T_0)}{T_{01} - (T_{0c} + \Delta T_0)}, \tag{8.50}$$

where T_m is the rotor metal temperature,

$$\Delta T_0 = \frac{1}{2} U_2^2/C_p.$$

Rodgers refers to tests that indicate the possibility of obtaining $\varepsilon = 0.30$ at the rotor tip section with a cooling flow of approximately 10% of the main gas flow. Since the cool and hot streams rapidly mix, effectiveness decreases with distance from the point of impingement. A model study of the heat transfer aspects of film-cooled radial-flow gas turbines is given by Metzger and Mitchell (1966).

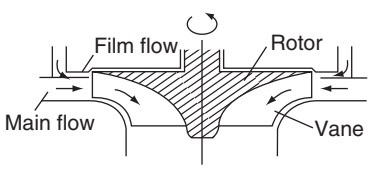

FIGURE 8.16

Cross-Section of Film-Cooled Radial Turbine

References

Abidat, M., Chen, H., Baines, N. C., and Firth, M. R. (1992). Design of a highly loaded mixed flow turbine. *Journal of Power and Energy, Proceedings of the Institution Mechanical Engineers*, *206*, 95–107.

Anon. (1971). Conceptual design study of a nuclear Brayton turboalternator-compressor. Contractor Report, General Electric Company. NASA CR-113925.

Balje, O. E. (1981). *Turbomachines—A Guide to Design, Selection and Theory*. New York: Wiley.

Benson, R. S. (1970). A review of methods for assessing loss coefficients in radial gas turbines. *International Journal of Mechanical Science*, *12*.

Benson, R. S., Cartwright, W. G., and Das, S. K. (1968). An investigation of the losses in the rotor of a radial flow gas turbine at zero incidence under conditions of steady flow. *Proceedings of the Institution Mechanical Engineers London*, *182*, Part 3H.

Dunham, J., and Panton, J. (1973). Experiments on the design of a small axial turbine. *Conference Publication 3, Institution of Mechanical Engineers*.

Glassman, A. J. (1976). Computer program for design and analysis of radial inflow turbines. NASA TN 8164.

Hiett, G. F., and Johnston, I. H. (1964). Experiments concerning the aerodynamic performance of inward radial flow turbines. *Proceedings of the Institution Mechanical Engineers*, *178*, Part 3I.

Huntsman, I., Hodson, H. P., and Hill, S. H. (1992). The design and testing of a radial flow turbine for aerodynamic research. *Journal of Turbomachinery, Transactions of the American Society of Mechanical Engineers*, *114*, p. 4.

Jamieson, A. W. H. (1955). The radial turbine. In: Sir H. Roxbee-Cox (ed.), *Gas Turbine Principles and Practice*, Chapter 9. London: Newnes.

Kearton, W. J. (1951). *Steam Turbine Theory and Practice* (6th ed.). New York: Pitman.

Kofskey, M. G., and Wasserbauer, C. A. (1966). Experimental performance evaluation of a radial inflow turbine over a range of specific speeds. NASA TN D-3742.

Meitner, P. L., and Glassman, J. W. (1983). Computer code for off-design performance analysis of radial-inflow turbines with rotor blade sweep. NASA TP 2199. AVRADCOM Technical Report 83-C-4.

Metzger, D. E., and Mitchell, J. W. (1966). Heat transfer from a shrouded rotating disc with film cooling. *Journal of Heat Transfer, Transactions of the American Society of Mechanical Engineers*, *88*.

Nusbaum, W. J., and Kofskey, M. G. (1969). Cold performance evaluation of 4.97 inch radial-inflow turbine designed for single-shaft Brayton cycle space-power system. NASA TN D-5090.

Rodgers, C. (1969). A cycle analysis technique for small gas turbines. *Technical Advances in Gas Turbine Design. Proceedings of the Institution Mechanical Engineers London*, *183*, Part 3 N.

Rodgers, C., and Geiser, R. (1987). Performance of a high-efficiency radial/axial turbine. *Journal of Turbomachinery, Transactions of the American Society of Mechanical Engineers*, *109*.

Rogers, G. F. C., and Mayhew, Y. R. (1995). *Thermodynamic and Transport Properties of Fluids* (5th ed.) Malden, MA: Blackwell.

Rohlik, H. E. (1968). Analytical determination of radial-inflow turbine design geometry for maximum efficiency. NASA TN D-4384.

Rohlik, H. E. (1975). Radial-inflow turbines. In: A. J. Glassman (ed.), *Turbine Design and Applications*. NASA SP 290, vol. 3.

Shepherd, D. G. (1956). *Principles of Turbomachinery*. New York: Macmillan.

Stanitz, J. D. (1952). Some theoretical aerodynamic investigations of impellers in radial and mixed flow centrifugal compressors. *Transactions of the American Society of Mechanical Engineers*, *74*, p. 4.

Stewart, W. L., Witney, W. J., and Wong, R. Y. (1960). A study of boundary layer characteristics of turbomachine blade rows and their relation to overall blade loss. *Journal of Basic Engineering, Transactions of the American Society of Mechanical Engineers*, *82*.

Whitfield, A. (1990). The preliminary design of radial inflow turbines. *Journal of Turbomachinery, Transactions of the American Society of Mechanical Engineers*, *112*, pp. 50–57.

Whitfield, A., and Baines, N. C. (1990). Computation of internal flows. In: A. Whitfield and N. C. Baines (eds.) *Design of Radial Turbomachines*, Chapter 8. New York: Longman.

Wilson, D. G., and Jansen, W. (1965). The aerodynamic and thermodynamic design of cryogenic radial-inflow expanders. ASME Paper 65—WA/PID-6, 1–13.

Wood, H. J. (1963). Current technology of radial-inflow turbines for compressible fluids. *Journal of Engineering and Power, Transactions of the American Society of Mechanical Engineers*, *85*.

PROBLEMS

1. A small inward radial flow gas turbine, comprising a ring of nozzle blades, a radial-vaned rotor and an axial diffuser, operates at the nominal design point with a total-to-total efficiency of 0.90. At turbine entry the stagnation pressure and temperature of the gas is 400 kPa and 1140 K. The flow leaving the turbine is diffused to a pressure of 100 kPa and has negligible final velocity. Given that the flow is just choked at nozzle exit, determine the impeller peripheral speed and the flow outlet angle from the nozzles. For the gas assume $\gamma = 1.333$ and $R = 287$ J/(kg°C).

2. The mass flow rate of gas through the turbine given in Problem 1 is 3.1 kg/s, the ratio of the rotor axial width–rotor tip radius (b_2/r_2) is 0.1 and the nozzle isentropic velocity ratio (ϕ_2) is 0.96. Assuming that the space between nozzle exit and rotor entry is negligible and ignoring the effects of blade blockage, determine

(i) the static pressure and static temperature at nozzle exit;
(ii) the rotor tip diameter and rotational speed;
(iii) the power transmitted assuming a mechanical efficiency of 93.5%.

3. A radial turbine is proposed as the gas expansion element of a nuclear powered Brayton cycle space power system. The pressure and temperature conditions through the stage at the design point are to be as follows:

Upstream of nozzles, $p_{01} = 699$ kPa, $T_{01} = 1145$ K;
Nozzle exit, $p_2 = 527.2$ kPa, $T_2 = 1029$ K;
Rotor exit, $p_3 = 384.7$ kPa, $T_3 = 914.5$ K; $T_{03} = 924.7$ K.

The ratio of rotor exit mean diameter to rotor inlet tip diameter is chosen as 0.49 and the required rotational speed as 24,000 rev/min. Assuming the relative flow at rotor inlet is radial and the absolute flow at rotor exit is axial, determine

(i) the total-to-static efficiency of the turbine;
(ii) the rotor diameter;
(iii) the implied enthalpy loss coefficients for the nozzles and rotor row.

The gas employed in this cycle is a mixture of helium and xenon with a molecular weight of 39.94 and a ratio of specific heats of 5/3. The universal gas constant is $R_0 = 8.314$ kJ/(kg-mol K).

4. A film-cooled radial inflow turbine is to be used in a high performance open Brayton cycle gas turbine. The rotor is made of a material able to withstand a temperature of 1145 K at a tip speed of 600 m/s for short periods of operation. Cooling air is supplied by the compressor that operates at a stagnation pressure ratio of 4 to 1, with an isentropic efficiency of 80%, when air is admitted to the compressor at a stagnation temperature of 288 K. Assuming that the effectiveness of the film cooling is 0.30 and the cooling air temperature at turbine entry is the same as that at compressor exit, determine the maximum permissible gas temperature at entry to the turbine. Take $\gamma = 1.4$ for the air. Take $\gamma = 1.333$ for the gas entering the turbine. Assume $R = 287$ J/(kgK) in both cases.

5. The radial inflow turbine in Problem 3 is designed for a specific speed Ω_s of 0.55 (rad). Determine

(i) the volume flow rate and the turbine power output;
(ii) the rotor exit hub and tip diameters;
(iii) the nozzle exit flow angle and the rotor inlet passage width–diameter ratio, b_2/D_2.

6. An inward flow radial gas turbine with a rotor diameter of 23.76 cm is designed to operate with a gas mass flow of 1.0 kg/s at a rotational speed of 38,140 rev/min. At the design condition the inlet stagnation pressure and temperature are to be 300 kPa and 727°C. The turbine is to be "cold" tested in a laboratory where an air supply is available only at the stagnation conditions of 200 kPa and 102°C.

(i) Assuming dynamically similar conditions between those of the laboratory and the projected design determine, for the "cold" test, the equivalent mass flow rate and the speed of rotation. Assume the gas properties are the same as for air.
(ii) Using property tables for air, determine the Reynolds numbers for both the hot and cold running conditions. The Reynolds number is defined in this context as

$$\mathrm{Re} = \rho_{01} N D^2 / \mu_{01},$$

where ρ_{01} and μ_{01} are the stagnation density and stagnation viscosity of the air, N is the rotational speed (rev/s), and D is the rotor diameter.

7. For the radial flow turbine described in the previous problem and operating at the prescribed "hot" design point condition, the gas leaves the exducer directly to the atmosphere at a pressure of 100 kPa and without swirl. The absolute flow angle at rotor inlet is 72° to the radial direction. The relative velocity w_3 at the mean radius of the exducer (which is one half of the rotor inlet radius r_2) is twice the rotor inlet relative velocity w_2. The nozzle enthalpy loss coefficient, $\zeta_N = 0.06$. Assuming the gas has the properties of air with an average value of $\gamma = 1.34$ (this temperature range) and $R = 287$ J/kg K, determine

(i) the total-to-static efficiency of the turbine;
(ii) the static temperature and pressure at the rotor inlet;
(iii) the axial width of the passage at inlet to the rotor;
(iv) the absolute velocity of the flow at exit from the exducer;
(v) the rotor enthalpy loss coefficient;
(vi) the radii of the exducer exit given that the radius ratio at that location is 0.4.

8. One of the early space power systems built and tested for NASA was based on the Brayton cycle and incorporated an IFR turbine as the gas expander. Some of the data available concerning the turbine are as follows:

Total-to-total pressure ratio (turbine inlet to turbine exit), $p_{01}/p_{03} = 1.560$;
Total-to-static pressure ratio, $p_{01}/p_3 = 1.613$;
Total temperature at turbine entry, $T_{01} = 1083$ K;
Total pressure at inlet to turbine, $T_{01} = 91$ kPa;
Shaft power output (measured on a dynamometer), $P_{\mathrm{net}} = 22.03$ kW;
Bearing and seal friction torque (a separate test), $\tau_f = 0.0794$ Nm;

Rotor diameter, $D_2 = 15.29$ cm;
Absolute flow angle at rotor inlet, $\alpha_2 = 72°$;
Absolute flow angle at rotor exit, $\alpha_3 = 0°$;
The hub to shroud radius ratio at rotor exit, $r_{3h/r3s = 0.35;}$
Ratio of blade speed to jet speed, $v = U_2/c_0 = 0.6958$;
(c_0 based on total-to-static pressure ratio.)

For reasons of crew safety, an inert gas argon ($R = 208.2$ J/(kg K), ratio of specific heats, $\gamma = 1.667$) was used in the cycle. The turbine design scheme was based on the concept of optimum efficiency. Determine, for the design point

(i) the rotor vane tip speed;
(ii) the static pressure and temperature at rotor exit;
(iii) the gas exit velocity and mass flow rate;
(iv) the shroud radius at rotor exit;
(v) the relative flow angle at rotor inlet;
(vi) the specific speed.

Note: The volume flow rate to be used in the definition of the specific speed is based on the rotor exit conditions.

9. What is meant by the term *nominal design* in connection with a radial flow gas turbine rotor? Sketch the velocity diagrams for a 90° IFR turbine operating at the nominal design point. At entry to a 90° IFR turbine the gas leaves the nozzle vanes at an absolute flow angle, α_2, of 73°. The rotor blade tip speed is 460 m/s and the relative velocity of the gas at rotor exit is twice the relative velocity at rotor inlet. The rotor mean exit diameter is 45% of the rotor inlet diameter. Determine,

(i) the exit velocity from the rotor;
(ii) the static temperature difference, $T_2 - T_3$, of the flow between nozzle exit and rotor exit.

Assume the turbine operates at the nominal design condition and that $C_p = 1.33$ kJ/kg K.

10. The initial design of an IFR turbine is to be based upon Whitfield's procedure for optimum efficiency. The turbine is to be supplied with 2.2 kg/s of air, a stagnation pressure of 250 kPa, a stagnation temperature of 800°C, and have an output power of 450 kW. At turbine exit the static pressure is 105 kPA. Assuming for air that $\gamma = 1.33$ and $R = 287$ J/kg K, determine the value of Whitfield's power ratio, S, and the total-to-static efficiency of the turbine.

11. By considering the theoretical details of Whitfield's design problem for obtaining the optimum efficiency of an IFR turbine show that the correct choice for the relationship of the rotor inlet flow angles is obtained from the following equation,

$$\tan\alpha_2 = \frac{\sin\beta_2}{1 - \cos\beta_2}.$$

and that a minimum stagnation Mach number at rotor inlet is obtained from:

$$M_{02}^2 = \left(\frac{S}{\gamma - 1}\right)\frac{2\cos\beta_2}{1 + \cos\beta_2}.$$

12. An IFR turbine rotor is designed with 13 vanes and is expected to produce 400 kW from a supply of gas heated to a stagnation temperature of 1100 K at a flow rate of 1.2 kg/s. Using Whitfield's optimum efficiency design method and assuming $\eta_{ts} = 0.85$, determine

(i) the overall stagnation pressure to static pressure ratio;
(ii) the rotor tip speed and inlet Mach number, M_2, of the flow.

Assume $C_p = 1.187$ kJ/kg K and $\gamma = 1.33$.

13. Another IFR turbine is to be built to develop 250 kW of shaft power from a gas flow of 1.1 kg/s. The inlet stagnation temperature, T_{01}, is 1050 K, the number of rotor blades is 13, and the outlet static pressure, p_3, is 102 kPa. At rotor exit the area ratio, $\nu = r_{3h}/r_{3s} = 0.4$, and the velocity ratio, $c_{m3}/U_2 = 0.25$. The shroud to rotor inlet radius, r_{3s}/r_2, is 0.4. Using the optimum efficiency design method, determine

(i) the power ratio, S, and the relative and absolute flow angles at rotor inlet;
(ii) the rotor blade tip speed;
(iii) the static temperature at rotor exit;
(iv) the rotor speed of rotation and rotor diameter.

Evaluate the specific speed, Ω_s. How does this value compare with the optimum value of specific speed determined in Figure 8.15?

14. Using the same input design data for the IFR turbine given in Problem 5 and given that the total-to-static efficiency is 0.8, determine

(i) the stagnation pressure of the gas at inlet;
(ii) the total-to-total efficiency of the turbine.

15. An IFR turbine is required with a power output of 300 kW driven by a supply of gas at a stagnation pressure of 222 kPa, at a stagnation temperature of 1100 K, and at a flow rate of 1.5 kg/s. The turbine selected by the engineer has 13 vanes and preliminary tests indicate it should have a total-to-static efficiency of 0.86. Based upon the optimum efficiency design method sketch the appropriate velocity diagrams for the turbine and determine

(i) the absolute and relative flow angles at rotor inlet;
(ii) the overall pressure ratio;
(iii) the rotor tip speed.

16. For the IFR turbine of the previous problem the following additional information is made available:

$$c_{m3}/U_2 = 0.25, w_3/w_2 = 2.0, r_{3s}/r_2 = 0.7 \text{ and } \nu = 0.4.$$

Again, based upon the optimum efficiency design criterion, determine,

(i) the rotor diameter and speed of rotation;
(ii) the enthalpy loss coefficients of the rotor and the nozzles given that the nozzle loss coefficient is (estimated) to be one quarter of the rotor loss coefficient.